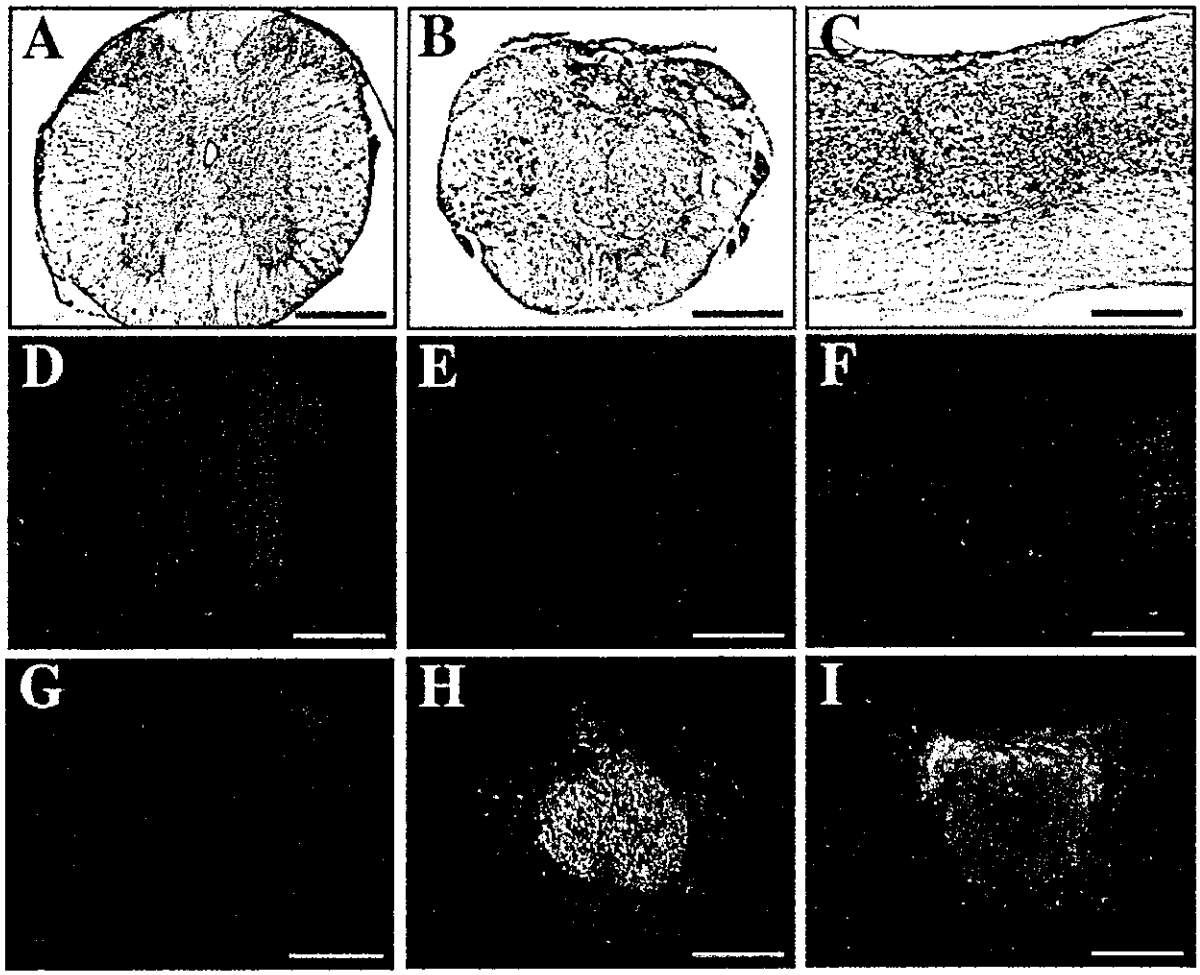

Fig. 2. Photomicrographs of representative immunohistochemistry and H&E-stained sections from the lesion epicenter 2 weeks after injury obtained from the MR16-1 group (B,C,E,F,H,I) and normal mice (A,D,G). **A–C:** H&E staining showed that the normal gray matter in the lesion epicenter had been completely replaced by a connective tissue scar. **D–F:** Distribution of Hu-immunoreactive cells (red) in normal and injured mice. The central lesion area was devoid of Hu-positive neurons. **G–I:** Mac-1 (CD11b)-immunoreactive cells were almost negative in the normal axial section (G), but they were aggregated mainly in the connective tissue scar area in injured spinal cord (H,I). A, B, D, E, G, and H, axial sections; C, F, and I, sagittal sections. Scale bars = 400 μm.

Behavioral Recovery

Given the histopathological improvements, such as the decreased astrogliosis and inflammatory cell infiltration, we investigated whether the histological changes were associated with better functional recovery by using three different behavioral tests. The mice in both the MR-16 group and the control group showed flaccid paralysis with no or little hindlimb movement throughout the first week after SCI, and this was followed by some recovery of hindlimb movement. To assess such functional recovery, we first examined a standardized open-field measure of locomotor function after the SCI, the BBB score, in which 21 is normal function and 0 is bilateral total paralysis of the hindlimbs. When BBB scoring is applied to mice, the size and speed of the hindpaws make it difficult to assign a precise score if the score exceeds 13 points (Ma et al., 2001), but that was not a problem in this study, because none of the mice had scores over 13 points (Jakeman et al., 2000). By 6 weeks after the injury, mice in the MR16-1 group had a significantly higher motor score (9.1 ± 0.5) than the control animals (6.4 ± 0.7), and the differences between the two groups 5 and 6 weeks after the injury were statistically significant (Fig. 7A). In the BBB score, 9 points represents the ability for hindlimb weight bearing. Even in mice, the difference of 8 points and 9 points was clearly detectable, because it was obvious whether they could bear weight or not.

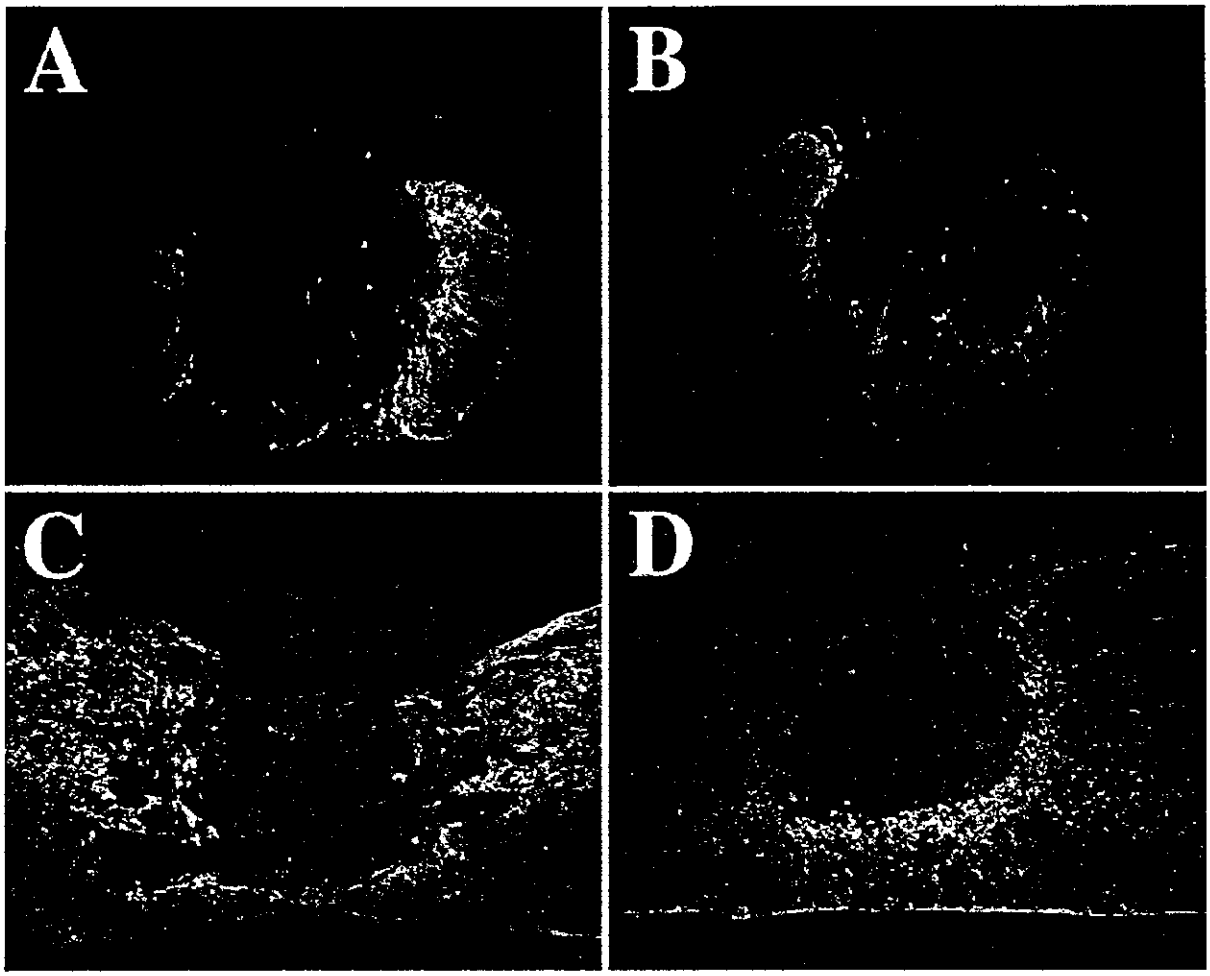

Fig. 3. Sections from the lesion epicenter of control mice (**A,C**) and MR16-1-treated mice (**B,D**) were counterstained with GFAP (green) and BrdU (red). The connective tissue scar area was almost completely GFAP negative but was surrounded with GFAP-positive astrocytes. This area in MR16-1-treated mice was smaller and astrogliosis around the central lesion was suppressed moderately compared with the control mice. A, B, axial sections; C, D, sagittal sections.

We then used a second assay employing SCANET, an automated motion-analysis system for measuring spontaneous motor activity (Shimosato and Ohkuma, 2000; Mikami et al., 2002), which is capable of assessing not only horizontal but also vertical movement. Vertical movement is an adequate index for assessment of locomotor function in spinal cord-injured mice. Mikami et al. (2002) even reported a statistically significant positive correlation between the RG score and the BBB Scale score. The vertical movement analysis revealed that 12 of the 15 mice in the MR16-1 group were able to rear more than once, whereas only 3 of the 15 mice were able to do so in the control group. The difference between the two groups was significant according to Fisher's exact probability test ($P < .05$). However, there were no significant differences in horizontal movements between the groups.

We performed the Rota-rod treadmill test to assess recovery of forelimb–hindlimb coordination. At low speed (5 rpm), there were statistically significant differences between the groups in average and maximum retention time in three trials at 5 and 6 weeks after the injury (Fig. 6B), but no differences were demonstrated at the middle speed (10 rpm) or high speed (15 rpm). These findings indicated that the recovery of forelimb–hindlimb coordination was poor even in the MR16-1 group, and they were consistent with the BBB scores, which never exceeded 12 points. In conclusion, MR16-1 group exhibited better functional recovery than the control mice in all three behavioral evaluations.

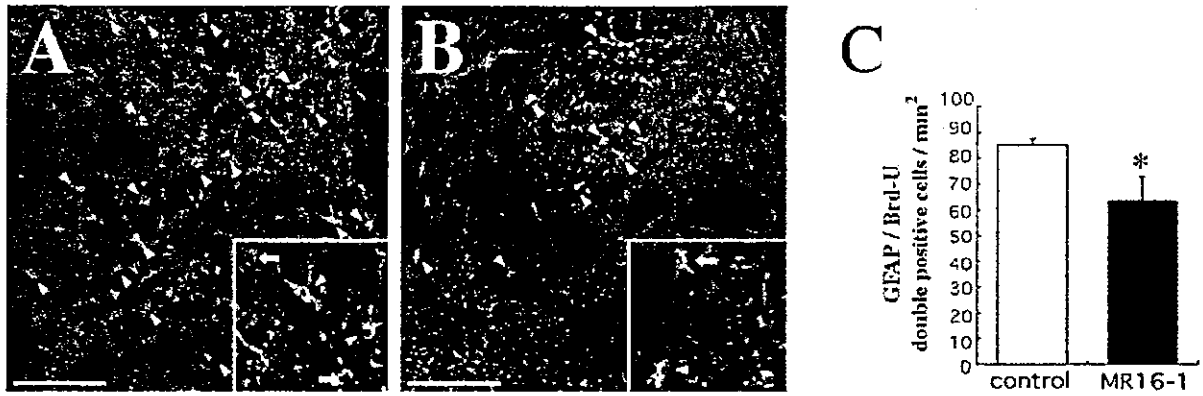

Fig. 4. MR16-1 suppressed the astrogliosis after SCI. **A,B:** Immunofluorescence staining for GFAP (green) and BrdU (red) at 2 weeks after the injury. Confocal imaging of the lesioned area with higher magnification in the control group (A) and MR16-1 group (B). **Insets:** Magnified views of A and B. Arrowheads point to a GFAP and BrdU double-positive cell, and the arrows point to GFAP-positive and BrdU-negative cells. **C:** Quantitative analysis of the average density of GFAP and BrdU double-positive cells at the lesion epicenter and 0.5 mm and 1.0 mm rostral and caudal to the epicenter in both groups. Values are means ± SEM. $*P < .05$; two-tailed *t*-test (n = 4 in the control group; n = 3 in the MR16-1 treated group). Scale bars = 40 μm.

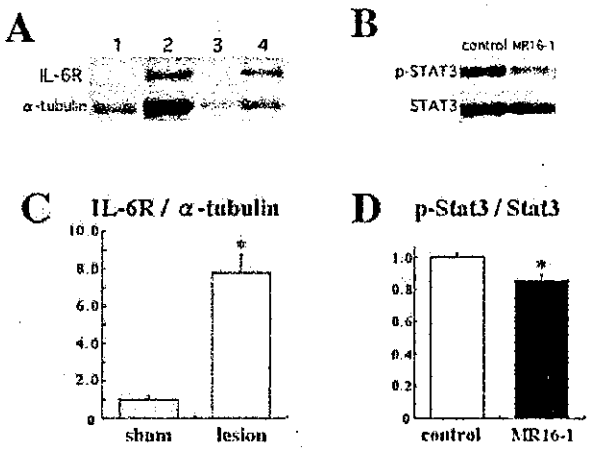

Fig. 5. Western blot analysis. **A,C:** Western blotting of soluble IL-6 receptor in the sham-operated spinal cord (lanes 1, 3) and lesioned spinal cord at 12 hr after the injury (lanes 2, 4). Quantification analysis revealed that the expression of IL-6R was 7.8-fold higher in the lesioned group at 12 hr after the injury compared with that in the sham group (n = 4 per each group). The average expression in the sham group was set as 1.0. $*P < .01$. **B,D:** The phosphorylated-STAT3 expression level in the spinal cord at 12 hr after the injury was quantitatively compared by Western blot analysis. The expression level of phosphorylated STAT3 in the MR16-1-treated group was 85.1% less compared with that in the control group. Values represent means ± SEM of the p-STAT3/STAT3 ratios (n = 4 per each group), with the average ratio in the control group set as 1.0. $*P < .05$.

DISCUSSION

Neutralization of soluble IL-6 receptor (sIL-6R) represents an attractive option for the treatment of several diseases characterized by excessive expression of IL-6, including B-cell neoplasia, rheumatoid arthritis, and autoimmune diseases (Yoshizaki et al., 1989; Takagi et al., 1998; Atreya et al., 2000). In this study, we first showed that the monoclonal anti-IL-6 receptor-α antibody MR16-1 blocked the IL-6 signaling that induced NSPCs to differentiate into astrocytes in vitro. Bonni et al. (1997) observed that activation of the gp130 signaling pathway selectively enhanced the differentiation of embryonic cerebral cortical precursor cells toward astrocytes, and we confirmed very similar effects of IL-6 signaling on NSPCs harvested from the spinal cord of adult mice.

Johansson et al. (1999) demonstrated that the endogenous NSPCs of adult spinal cord proliferate rapidly and differentiate exclusively into astrocytes in response to injury. Although the precise mechanism of this restrictive differentiation of NSPCs remains to be elucidated, activation of IL-6 signaling could be one of the major contributions of such selective astrocytic differentiation after SCI. IL-6 expression increases dramatically during the acute phase of SCI and then declines sharply within a few days (Hostettler and Carlson, 2002; Pan et al., 2002; Nakamura et al., 2003), and we confirmed the increase in sIL-6R (Yan et al., 1992) after SCI by Western blot analysis (Fig. 5A,C). This up-regulation of IL-6 signaling in the acute phase would be closely associated with glial scar formation after SCI (for review see Okano, 2002; Okano et al., 2003). Klein et al. (1997) show a massive reduction in the number of activated GFAP-positive astrocytes when the facial nerve of IL-6-deficient mice was transected, and Brunello et al. (2000) demonstrated massive reactive gliosis with numerous GFAP-immunoreactive astrocytes in all parts of the CNS in uninjured IL-6/sIL-6R double-transgenic mice. Therefore, we hypothesized that the astrogliosis could be suppressed by blocking IL-6 signaling after

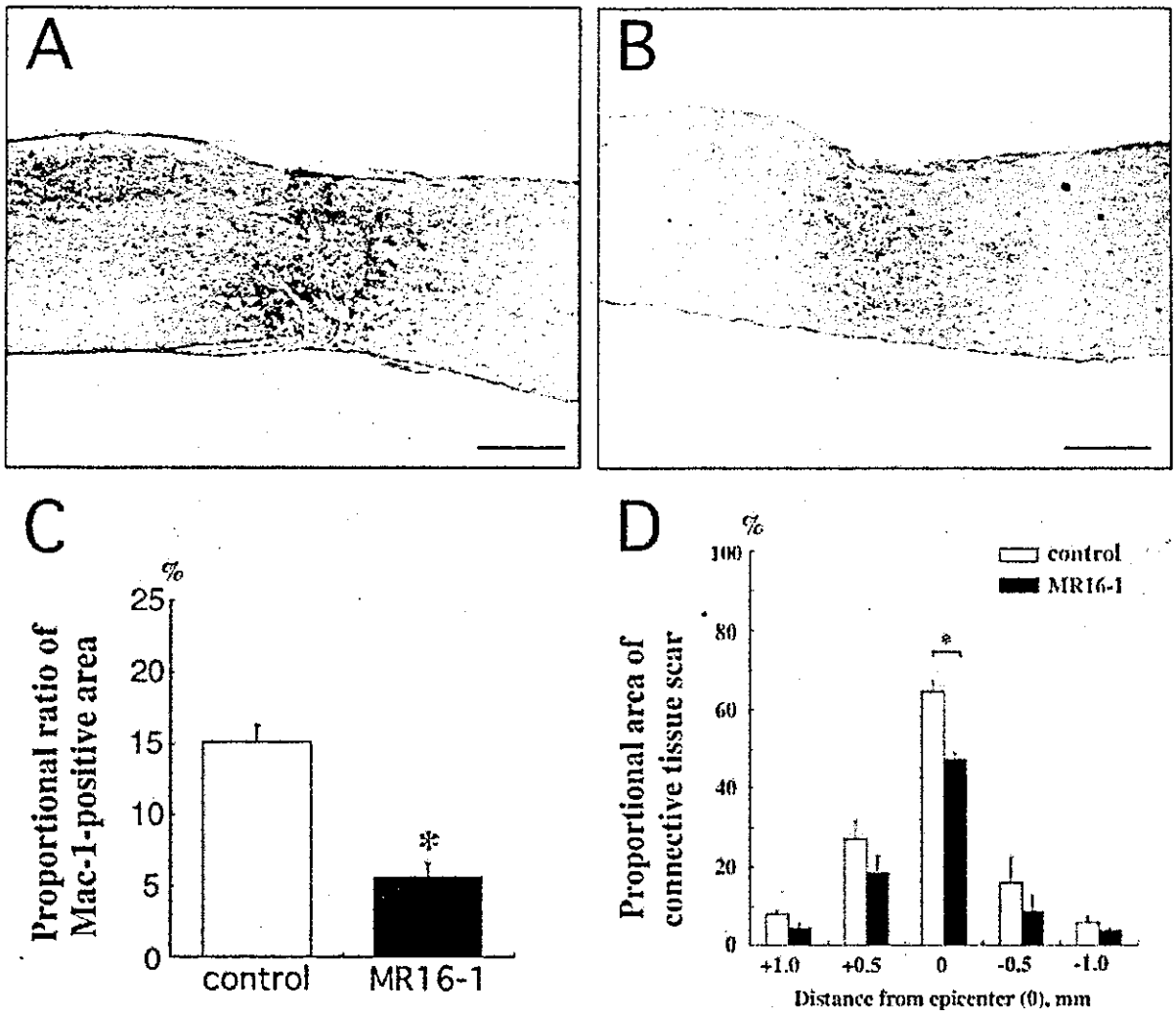

Fig. 6. Inflammatory responses were markedly decreased by MR16-1. **A,B:** Immunolabeling of Mac-1-positive cells in injured spinal cord at 2 weeks after injury. Representative sagittal section at the lesion epicenter from the control group (A) and the M16-1 group (B). **C:** Measurement of the area of Mac-1 immiunoreactivity in 3-mm sagittal sections from both groups. The immunolabeled area was significantly smaller in the MR16-1 group than in the control group. Values are means ± SEM. $*P < .05$; two-tailed t-test (n = 4 in the control group; n = 3 in the MR16-1 group). **D:** The area of the connective tissue scar as a percentage of the total axial area was calculated at the lesion epicenter and 0.5 and 1.0 mm rostral and caudal to the epicenter in both groups. The connective tissue scar area in the epicenter was significantly smaller in the MR16-1 mice. Values are means ± SEM. $*P < .05$; two-tailed t-test (n = 4 per each group). Scale bars = 500 μm.

SCI in vivo. In the present study, we showed a 15% decrease of phosphorylated-STAT3 expression at 12 hr after the injury and a 25% decrease in the number of GFAP and BrdU double-positive cells at 2 weeks after injury with systemic administration of MR16-1, compared with the control animals, suggesting that astrogliosis and IL-6 signaling are closely related. However, the precise mechanism regulating astrogliosis remains to be elucidated. In the present study, we were not able to determine the extent to which endogenous multipotential progenitors or resident astrocytes contributed to the $GFAP^+/BrdU^+$ cells. Kernie et al. (2001), however, reported that a significant amount of the astrogliotic scar formed after an injury is attributable to newly generated astrocytes and not to activation or migration of resident astrocytes.

Glial scar formation is considered a major cause of the poor regeneration after adult CNS after injury. A

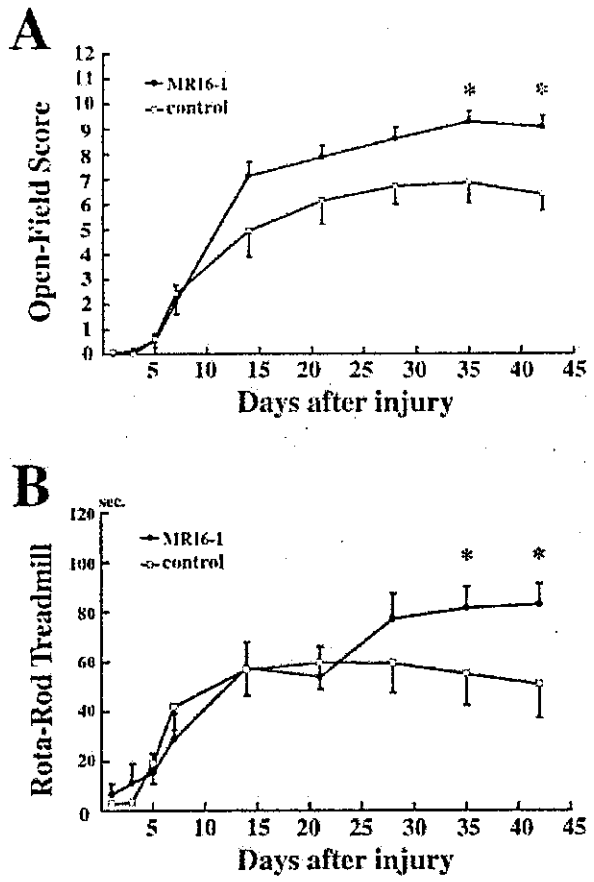

Fig. 7. Effect of MR16-1 on functional recovery. A: BBB scores in the control group (n = 15) and MR16-1 group (n = 15) were evaluated over a 6-week period. B: Retention time on the rotating rod in the control group (n = 15) and MR16-1 group (n = 15) at a speed of 5 rpm. Squares represent control mice, and circles represent MR16-1-treated mice. Values are means ± SEM. $*P < .05$; two-tailed t-test.

recent study reported that glial scars and associated extracellular matrix inhibit axonal regeneration with several molecules, such as chondroitin sulfate proteoglycans, tenascin, brevican, and neurocan (Fawcett and Asher, 1999). Bradbury et al. (2002) also demonstrated that degradation of chondroitin sulfate proteoglycans that are contained in glial scars at injury site with chondroitinase ABC improved functional recovery and promoted regeneration of both ascending sensory projections and descending long tract axons. Thus, modulating astrogliosis is a rational target for treating spinal cord injury and enhancing axonal regeneration, resulting in functional recovery (McGraw et al., 2001). Ridet et al. (2000) reported that suppression of glial scar formation with a 2-Gy dose of radiation after injury also improved functional recovery. In the present study, we demonstrated that administration of MR16-1 promoted functional recovery in three different behavioral evaluations (Fig. 7). Although further investigations are required, one possible explanation for the observed functional recovery is that the suppression of astrogliosis by MR16-1 treatment reduced the expression of glial scar-derived inhibitory molecules against axonal regeneration, which promoted axonal regeneration after injury.

Manipulation of inflammatory responses is another therapeutic strategy for SCI. Although the precise functions and effects of inflammatory cells after injury have not been completely elucidated, previous studies have suggested that inflammatory responses spread the damage to surrounding tissue, induce apoptotic cell death, and impair spontaneous regeneration and functional recovery (Carlson et al., 1998; Popovich and Jones, 2003). Several approaches to protecting the injured spinal cord from secondary pathological processes, such as the antiinflammatory cytokine IL-10, erythropoietin, matrix metalloprotease inhibitor, and methylprednisolone, have been assessed and been demonstrated to be effective, even in terms of functional recovery (Bracken et al., 1997; Bethea et al., 1999; Gorio et al., 2002; Nobel et al., 2002). IL-6 is one of the principal proinflammatory cytokines; it plays roles in regulating various steps in inflammatory reactions, i.e., activation and infiltration by neutrophils, monocytes, macrophages, and lymphocytes (Van Wagoner and Benveniste, 1999; Leskovar et al., 2000). The number of inflammatory cells is significantly correlated with the amount of tissue damage at each level (Carlson et al., 1998), and the size of the CTS, which is the characteristic lesion of contusive SCI in mice, as opposed to central cavitation in rats, correlates with the severity of the injury (Ma et al., 2001). We tested, based on these studies, our hypothesis that MR16-1 would suppress the inflammatory response after injury by assessing the extent of Mac-1-positive inflammatory cell infiltration and measuring the area of the CTS. The results demonstrated that fewer Mac-1-positive cells infiltrated both the gray and the white matter and that the CTS area at the lesion epicenter was significantly smaller in the MR16-1 group than in the control group (Fig. 6). This modulation of the inflammatory response after injury by administration of MR16-1 probably attenuated the tissue damage and secondary neural destruction and caused the functional recovery demonstrated in the present study (Fig. 7). Our findings are consistent with the results of previous studies suggesting that administration of proinflammatory cytokines at lesion sites 1 day after an injury increases the recruitment and activation of macrophages, neutrophils, and microglial cells (Klusman and Schwab, 1997) and that delivery of IL-6/sIL-6R fusion protein to injury sites induces a sixfold increase in neutrophils and a twofold increase of macrophages and microglial cells (Lacroix et al., 2002).

By contrast, IL-6 exerts multiple effects in the CNS, and several experiments have shown the neuronal protective and outgrowth effects of IL-6 signaling. For example, Marz et al. (1998) showed that IL-6 signaling enhances neuronal survival in rat sympathetic neurons, and Hirota et

al. (1996) observed accelerated regeneration of the axotomized hypoglossal nerve in transgenic mice constitutively expressing IL-6 and IL-6R. Administration of IL-6 to animals with cerebral ischemia reduced tissue damage and prevented learning disabilities in vivo (Matsuda et al., 1996; Loddick et al., 1998). In SCI, however, delivery of IL-6/sIL-6R fusion protein (hyper-IL-6) to the lesion site induced a fourfold decrease in axonal outgrowth, which indicated that the neurotrophic effects of IL-6 were overwhelmed by its proinflammatory features in vivo (Lacroix et al., 2002). These clear differences in IL-6 effect may depend on the level and timing of its expression. Although the role of IL-6 signaling seemed to be complex and well regulated in accordance with the physiopathology, we wish to emphasize the neurotoxic effect of IL-6, at least in the acute phase after SCI. We also confirmed by ELISA (data not shown) that the half-life of MR16-1 is about 3 days in injured mice, so the kinetics of MR16-1 would produce an ideal effect, because it suppresses excess IL-6 signaling only in the acute phase and dose not interfere the neuroprotective effect in the subacute and chronic phases.

A critical merit of this sIL-6R antibody is that humanized antibody to human IL-6R (MRA; Atlizumab) has already been reshaped (Sato et al., 1993), and its therapeutic efficacy has been confirmed in clinical trials in several diseases, including rheumatoid arthritis, Castleman's disease, and multiple myeloma (Sato et al., 1993; Nishimoto et al., 2000; Choy et al., 2002). The Phase II clinical trial in rheumatoid arthritis has already been completed in Japan and Europe, and safety, tolerability, antigenicity, pharmacokinetics, and efficacy have been demonstrated. Although the data reported here are preliminary, they suggest that blockage of IL-6 signaling may be beneficial in patients with acute SCI. In summary, the results of this study show that a single dose of anti-mouse IL-6R monoclonal antibody enhances functional recovery after SCI in adult mice, probably by attenuating inflammatory response, secondary tissue damage, and astrogliosis.

ACKNOWLEDGMENTS

We thank Drs. K. Shiba and T. Ueta (Spina Cord Injury Center, Fukuoka, Japan) for their continuous encouragement and valuable discussions. This work was supported by grants from the Japanese Ministry of Education, Culture, Sports, Science and Technology and the Japan Science and Technology Corporation (CREST) to H.O., and a Grant-in-Aid for the 21st Century COE (Center of Excellence) program to Keio University from the Japanese Ministry of Education, Culture, Sports, Science and Technology.

REFERENCES

Atreya R, Mudter J, Finotto S, Mullberg J, Jostock T, Wirtz S, Schutz M, Bartsch B, Holtmann M, Becker C, Strand D, Czaja J, Schlaak JF, Lehr HA, Autschbach F, Schurmann G, Nishimoto N, Yoshizaki K, Ito H, Kishimoto T, Galle PR, Rose-John S, Neurath MF. 2000. Blockade of interleukin 6 trans signaling suppresses T-cell resistance against apoptosis in chronic intestinal inflammation: evidence in crohn disease and experimental colitis in vivo. Nat Med 6:583–588.

Basso DM, Beattie MS, Bresnahan JC. 1996. Graded histological and locomotor outcomes after spinal cord contusion using the NYU weight-drop device versus transection. Exp Neurol 139:244–256.

Bethea JR, Nagashima H, Acosta MC, Briceno C, Gomez F, Marcillo AE, Loor K, Green J, Dietrich WD. 1999. Systemically administered interleukin-10 reduces tumor necrosis factor-alpha production and significantly improves functional recovery following traumatic spinal cord injury in rats. J Neurotrauma 16:851–863.

Bjorklund A, Lindvall O. 2000. Self-repair in the brain. Nature 405:892–895.

Bonni A, Sun Y, Nadal-Vicens M, Bhatt A, Frank DA, Rozovsky I, Stahl N, Yancopoulos GD, Greenberg ME. 1997. Regulation of gliogenesis in the central nervous system by the JAK-STAT signaling pathway. Science 278:477–483.

Bracken MB, Shepard MJ, Holford TR, Leo-Summers L, Aldrich EF, Fazl M, Fehlings M, Herr DL, Hitchon PW, Marshall LF, Nockels RP, Pascale V, Perot PL Jr, Piepmeier J, Sonntag VK, Wagner F, Wilberger JE, Winn HR, Young W. 1997. Administration of methylprednisolone for 24 or 48 hr or tirilazad mesylate for 48 hr in the treatment of acute spinal cord injury. Results of the Third National Acute Spinal Cord Injury Randomized Controlled Trial. National Acute Spinal Cord Injury Study. JAMA 277:1597–1604.

Bradbury EJ, Moon LD, Popat RJ, King VR, Bennett GS, Patel PN, Fawcett JW, McMahon SB. 2002. Chondroitinase ABC promotes functional recovery after spinal cord injury. Nature 416:636–640.

Brunello AG, Weissenberger J, Kappeler A, Vallan C, Peters M, Rose-John S, Weis J. 2000. Astrocytic alterations in interleukin-6/soluble interleukin-6 receptor alpha double-transgenic mice. Am J Pathol 157: 1485–1493.

Carlson SL, Parrish ME, Springer JE, Doty K, Dossett L. 1998. Acute inflammatory response in spinal cord following impact injury. Exp Neurol 151:77–88.

Choy EH, Isenberg DA, Garrood T, Farrow S, Ioannou Y, Bird H, Cheung N, Williams B, Hazleman B, Price R, Yoshizaki K, Nishimoto N, Kishimoto T, Panayi GS. 2002. Therapeutic benefit of blocking interleukin-6 activity with an anti-interleukin-6 receptor monoclonal antibody in rheumatoid arthritis: a randomized, double-blind, placebo-controlled, dose-escalation trial. Arthritis Rheum 46:3143–3150.

David S, Lacroix S. 2003. Molecular approaches to spinal cord repair. Annu Rev Neurosci 26:411–440.

Fawcett JW, Asher RA. 1999. The glial scar and central nervous system repair. Brain Res Bull 49:377–391.

Gorio A, Gokmen N, Erbayraktar S, Yilmaz O, Madaschi L, Cichetti C, Di Giulio AM, Vardar E, Cerami A, Brines M. 2002. Recombinant human erythropoietin counteracts secondary injury and markedly enhances neurological recovery from experimental spinal cord trauma. Proc Natl Acad Sci USA 99:9450–9455.

Gruner JA. 1992. A monitored contusion model of spinal cord injury in the rat. J Neurotrauma 9:123–128.

Hirota H, Kiyama H, Kishimoto T, Taga T. 1996. Accelerated nerve regeneration in mice by upregulated expression of interleukin (IL) 6 and IL-6 receptor after trauma. J Exp Med 183:2627–2634.

Horner PJ, Power AE, Kempermann G, Kuhn HG, Palmer TD, Winkler J, Thal LJ, Gage FH. 2000. Proliferation and differentiation of progenitor cells throughout the intact adult rat spinal cord. J Neurosci 20:2218–2228.

Hostettler ME, Carlson SL. 2002. PAF antagonist treatment reduces pro-inflammatory cytokine mRNA after spinal cord injury. Neuroreport 13:21–24.

Jakeman LB, Guan Z, Wei P, Ponnappan R, Dzwonczyk R, Popovich PG, Stokes BT. 2000. Traumatic spinal cord injury produced by controlled contusion in mouse. J Neurotrauma 17:299–319.

Johansson CB, Momma S, Clarke DL, Risling M, Lendahl U, Frisen J. 1999. Identification of a neural stem cell in the adult mammalian central nervous system. Cell 96:25–34.

Katsume A, Saito H, Yamada Y, Yorozu K, Ueda O, Akamatsu KI, Nishimoto N, Kishimoto T, Yoshizaki K, Ohsugi Y. 2002. Anti-interleukin 6 (IL-6) receptor antibody suppresses castleman's disease like symptoms emerged in IL-6 transgenic mice. Cytokine 20:304–311.

Kernie SG, Erwin TM, Parada LF. 2001. Brain remodeling due to neuronal and astrocytic proliferation after controlled cortical injury in mice. J Neurosci Res 66:317–326.

Klein MA, Moller JC, Jones LL, Bluethmann H, Kreutzberg GW, Raivich G. 1997. Impaired neuroglial activation in interleukin-6 deficient mice. Glia 19:227–233.

Klusman I, Schwab ME. 1997. Effects of pro-inflammatory cytokines in experimental spinal cord injury. Brain Res 762:173–184.

Kuhn PL, Wrathall JR. 1998. A mouse model of graded contusive spinal cord injury. J Neurotrauma 15:125–140.

Lacroix S, Chang L, Rose-John S, Tuszynski MH. 2003. Delivery of hyper-interleukin-6 to the injured spinal cord increases neutrophil and macrophage infiltration and inhibits axonal growth. J Comp Neurol 454:213–228.

Leskovar A, Moriarty LJ, Turek JJ, Schoenlein IA, Borgens RB. 2000. The macrophage in acute neural injury: changes in cell numbers over time and levels of cytokine production in mammalian central and peripheral nervous systems. J Exp Biol 203:1783–1795.

Loddick SA, Turnbull AV, Rothwell NJ. 1998. Cerebral interleukin-6 is neuroprotective during permanent focal cerebral ischemia in the rat. J Cereb Blood Flow Metab 18:176–179.

Ma M, Basso DM, Walters P, Stokes BT, Jakeman LB. 2001. Behavioral and histological outcomes following graded spinal cord contusion injury in the C57Bl/6 mouse. Exp Neurol 169:239–254.

Marz P, Cheng JG, Gadient RA, Patterson PH, Stoyan T, Otten U, Rose-John S. 1998. Sympathetic neurons can produce and respond to interleukin 6. Proc Natl Acad Sci USA 95:3251–3256.

Matsuda S, Wen TC, Morita F, Otsuka H, Igase K, Yoshimura H, Sakanaka M. 1996. Interleukin-6 prevents ischemia-induced learning disability and neuronal and synaptic loss in gerbils. Neurosci Lett 204:109–112.

McGraw J, Hiebert GW, Steeves JD. 2001. Modulating astrogliosis after neurotrauma. J Neurosci Res 63:109–115.

Meima L, Moran P, Matthews W, Caras IW. 1997. Lerk2 (ephrin-B1) is a collapsing factor for a subset of cortical growth cones and acts by a mechanism different from AL-1 (ephrin-A5). Mol Cell Neurosci 9:314–328.

Mikami Y, Toda M, Watanabe M, Nakamura M, Toyama Y, Kawakami Y. 2002. A simple and reliable behavioral analysis of locomotor function after spinal cord injury in mice. Technical note. J Neurosurg 97:142–147.

Nakamura M, Houghtling RA, McArthur L, Bayer BM, Bregman BS. 2003. Difference in cytokine gene expression profile between acute and secondary injury in adult rat spinal cord. Ex Neurol 184:313–325.

Nakashima K, Yanagisawa M, Arakawa H, Kimura N, Hisatsune T, Kawabata M, Miyazono K, Taga T. 1999. Synergistic signaling in fetal brain by STAT3-Smad1 complex bridged by p300. Science 284:479–482.

Nishimoto N, Sasai M, Shima Y, Nakagawa M, Matsumoto T, Shirai T, Kishimoto T, Yoshizaki K. 2000. Improvement in Castleman's disease by humanized anti-interleukin-6 receptor antibody therapy. Blood 95:56–61.

Noble LJ, Donovan F, Igarashi T, Goussev S, Werb Z. 2002. Matrix metalloproteinases limit functional recovery after spinal cord injury by modulation of early vascular events. J Neurosci 22:7526–7535.

Ogura H, Matsumoto M, Mikoshiba K. 2001. Motor discoordination in mutant mice heterozygous for the type 1 inositol 1,4,5-trisphosphate receptor. Behav Brain Res 122:215–219.

Ohtani T, Ishihara K, Atsumi T, Nishida K, Kaneko Y, Miyata T, Itoh S, Narimatsu M, Maeda H, Fukada T, Itoh M, Okano H, Hibi M, Hirano T. 2000. Dissection of signaling cascades through gp130 in vivo: reciprocal roles for STAT3- and SHP2-mediated signals in immune responses. Immunity 12:95–105.

Okano H. 2002. Stem cell biology of the central nervous system. J Neurosci Res 69:698–707.

Okano H, Ogawa Y, Nakamura M, kaneko S, Iwanami A, Toyama Y. 2003. Transplantation of neural stem cells into the spinal cord after injury. Semin Cell Dev Biol 14:191–198.

Okazaki M, Yamada Y, Nishimoto N, Yoshizaki K, Mihara M. 2002. Characterization of anti-mouse interleukin-6 receptor antibody. Immunol Lett 84:231–240.

Pan JZ, Ni L, Sodhi A, Aguanno A, Young W, Hart RP. 2002. Cytokine activity contributes to induction of inflammatory cytokine mRNAs in spinal cord following contusion. J Neurosci Res 68:315–322.

Popovich PG, Jones TB. 2003. Manipulating neuroinflammatory reactions in the injured spinal cord: back to basics. Trends Pharmacol Sci 24:13–17.

Reynolds BA, Tetzlaff W, Weiss S. 1992. A multipotent EGF-responsive striatal embryonic progenitor cell produces neurons and astrocytes. J Neurosci 12:4565–4574.

Ridet JL, Pencalet P, Belcram M, Giraudeau B, Chastang C, Philippon J, Mallet J, Privat A, Schwartz L. 2000. Effects of spinal cord X-irradiation on the recovery of paraplegic rats. Exp Neurol 161:1–14.

Romano M, Sironi M, Toniatti C, Polentarutti N, Fruscella P, Ghezzi P, Faggioni R, Luini W, van Hinsbergh V, Sozzani S, Bussolino F, Poli V, Ciliberto G, Mantovani A. 1997. Role of IL-6 and its soluble receptor in induction of chemokines and leukocyte recruitment. Immunity 6:315–325.

Sato K, Tsuchiya M, Saldanha J, Koishihara Y, Ohsugi Y, Kishimoto T, Bendig MM. 1993. Reshaping a human antibody to inhibit the interleukin 6-dependent tumor cell growth. Cancer Res 53:851–856.

Shimazaki T, Shingo T, Weiss S. 2001. The ciliary neurotrophic factor/leukemia inhibitory factor/gp130 receptor complex operates in the maintenance of mammalian forebrain neural stem cells. J Neurosci 21:7642–7653.

Shimosato K, Ohkuma S. 2000. Simultaneous monitoring of conditioned place preference and locomotor sensitization following repeated administration of cocaine and methamphetamine. Pharmacol Biochem Behav 66:285–292.

Taga T, Kishimoto T. 1997. Gp130 and the interleukin-6 family of cytokines. Annu Rev Immunol 15:797–819.

Taga T, Hibi M, Hirata Y, Yamasaki K, Yasukawa K, Matsuda T, Hirano T, Kishimoto T. 1989. Interleukin-6 triggers the association of its receptor with a possible signal transducer, gp130. Cell 58:573–581.

Takagi N, Mihara M, Moriya Y, Nishimoto N, Yoshizaki K, Kishimoto T, Takeda Y, Ohsugi Y. 1998. Blockage of interleukin-6 receptor ameliorates joint disease in murine collagen-induced arthritis. Arthritis Rheum 41:2117–2121.

Takahashi M, Arai Y, Kurosawa H, Sueyoshi N, Shirai S. 2003. Ependymal cell reactions in spinal cord segments after compression injury in adult rat. J Neuropathol Exp Neurol 62:185–194.

Tamura T, Udagawa N, Takahashi N, Miyaura C, Tanaka S, Yamada Y, Koishihara Y, Ohsugi Y, Kumaki K, Taga T. 1993. Soluble interleukin-6 receptor triggers osteoclast formation by interleukin 6. Proc Natl Acad Sci USA 90:11924–11928.

Tuna M, Polat S, Erman T, Ildan F, Gocer AI, Tuna N, Tamer L, Kaya M, Cetinalp E. 2001. Effect of anti-rat interleukin-6 antibody after spinal cord injury in the rat: inducible nitric oxide synthase expression, sodium- and potassium-activated, magnesium-dependent adenosine-5'-triphosphatase and superoxide dismutase activation, and ultrastructural changes. J Neurosurg 95:64–73.

Van Wagoner NJ, Benveniste EN. 1999. Interleukin-6 expression and regulation in astrocytes. J Neuroimmunol 100:124–139.

Yan HQ, Banos MA, Herregodts P, Hooghe R, Hooghe-Peters EL. 1992. Expression of interleukin (IL)-1 beta, IL-6 and their respective receptors in the normal rat brain and after injury. Eur J Immunol 22:2963–7291.

ELSEVIER

MCN Molecular and Cellular Neuroscience

www.elsevier.com/locate/ymcne
Mol. Cell. Neurosci. 26 (2004) 258–270

Downregulation of STAT3 activation is required for presumptive rod photoreceptor cells to differentiate in the postnatal retina

Yoko Ozawa,[a,b] Keiko Nakao,[a,c] Takuya Shimazaki,[a,c] Junji Takeda,[d] Shizuo Akira,[e] Katsuhiko Ishihara,[f] Toshio Hirano,[f,g] Yoshihisa Oguchi,[b] and Hideyuki Okano[a,c,*]

[a] *Department of Physiology, Keio University School of Medicine, Shinjuku, Tokyo 160-8582, Japan*
[b] *Department of Ophthalmology, Keio University School of Medicine, Shinjuku, Tokyo 160-8582, Japan*
[c] *Core Research for Evolutional Science and Technology (CREST), Japan Science and Technology Corporation (JST), Honcho, Kawaguchi, Saitama 332-0012, Japan*
[d] *Collaborative Research Center for Advanced Science and Technology and Department of Social and Environmental Medicine, Graduate School of Medicine, Osaka University, Suita, Osaka 565-0871, Japan*
[e] *Department of Host Defense, Research Institute for Microbial Diseases, Osaka University, Suita, Osaka 565-0871, Japan*
[f] *Laboratory of Developmental Immunology, Graduate School of Frontier Biosciences, Osaka University, Suita, Osaka 565-0871, Japan*
[g] *Laboratory for Cytokine Signaling, RIKEN Research Center for Allergy and Immunology, Tsurumi, Yokohama City, Kanagawa 230-0045, Japan*

Received 28 July 2003; revised 10 February 2004; accepted 10 February 2004

Available online 17 April 2004

Ciliary neurotrophic factor (CNTF) has been known to inhibit the differentiation of presumptive rod photoreceptor cells; however, the underlying mechanisms have remained to be elucidated. We demonstrated that STAT3 activation, but not SHP2 activation, is responsible for the CNTF/gp130 signaling that inhibits expression of Rhodopsin and its upstream activator, *crx*, in the retinal explants derived from P0 mice (P0 retinal explants), utilizing STAT3-deficient retina and electroporation of dominant-negative form of STAT3 (STAT3F). We also demonstrated that STAT3 activation in presumptive rod photoreceptor cells at E18.5 is rapidly downregulated at P0, when Rhodopsin expression starts during retinal development. Persistent STAT3 activation in the P0 retinal explants prevented Rhodopsin expression and rapid upregulation of *crx* expression. STAT3-deficient retinas did not exhibit precocious rod photoreceptor cell differentiation as a whole, although they occasionally exhibited precocious upregulation of *crx* mRNA. Thus, we conclude that downregulation of STAT3 activation is required, but insufficient, for rod photoreceptor cell differentiation in the postnatal retina.

Introduction

It is well known that retinal cell differentiation occurs sequentially during the perinatal period, extending from the late embryonic period to the early postnatal period, so that the composition and arrangement of each cell type are well organized within the neural retina (Cepko et al., 1996; Livesey and Cepko, 2001). However, since there are considerable overlaps between the birth dates of the different cell types (Morrow et al., 1998a,b), there must be some regulatory mechanisms that strictly control the timing of differentiation of postmitotic cells. Presumptive rod photoreceptor cells first appear to exit cell cycle in the late embryonic period in rodent, for instance at E15 in rat retina, and then gradually increase in number (Morrow et al., 1998a,b), in the outer neuroblastic layer (onbl), and later in the outer nuclear layer (ONL). However, expression of Rhodopsin, one of the terminal differentiation markers for rod photoreceptor cells, only begins in the early postnatal period. Previous studies have shown that differentiation of rod photoreceptor cells is to some extent influenced by extrinsic diffusible factors (Altshuler and Cepko, 1992; Altshuler et al., 1993; Kelley et al., 1994; Levine et al., 2000; Lillien, 1995). One of the factors that inhibit rod photoreceptor cell differentiation is reported to be present at a high level in the embryonic retina but downregulated in the postnatal retina, and that factor has been demonstrated to be ciliary neurotrophic factor (CNTF) (Belliveau et al., 2000; Ezzeddine et al., 1997; Kirsch et al., 1998; Levine et al., 2000; Neophytou et al., 1997; Schulz-Key et al., 2002). Since CNTF is present at a high level in the embryonic retina (Kirsch et al., 1997) and downregulated in the early postnatal retina (Kirsch et al., 1997; Schulz-Key et al., 2002), inhibition by CNTF is one of the potential explanations for the lag in rod photoreceptor cell differentiation after cell cycle withdrawal in the embryonic period.

On the other hand, intrinsic regulatory mechanisms (Morrow et al., 1998a; Watanabe and Raff, 1990) involving transcription factors that activate a particular set of terminal marker genes also play important roles in the differentiation of each type of retinal cells. One of the essential transcription factors in activating *rhodopsin* expression is the homeodomain protein, Crx (Chen et al., 1997; Furukawa et al., 1997, 1999, 2002; Livesey et al., 2000). Thus, *crx* should be upregulated to induce rod photoreceptor cell differentiation.

Based on the above, an appropriate combination of extrinsic and intrinsic factors is thought to be necessary for each subset of

* Corresponding author. Department of Physiology, Keio University School of Medicine, Shinanomichi, Shinjuku 160 8582, Tokyo, Japan. Fax: +81-3-3357-5445.
E-mail address: hidokano@sc.itc.keio.ac.jp (H. Okano).
Available online on ScienceDirect (www.sciencedirect.com.)

1044-7431/$ - see front matter © 2004 Elsevier Inc. All rights reserved.
doi:10.1016/j.mcn.2004.02.001

retinal cells to differentiate (Cepko et al., 1996; Edlund and Jessell, 1999; Harris, 1997; Livesey and Cepko, 2001; Watanabe and Raff, 1990). But the underlying mechanisms, especially the interaction between extrinsic and intrinsic factors, still remain to be elucidated. Although CNTF/gp130 is known to function through at least two signaling pathways, that is, the JAK/STAT pathway and the SHP2-RAS/MAPK pathway, no specific mechanism has been assigned to its inhibition of rod photoreceptor cell differentiation.

In this study, we demonstrated that CNTF/gp130 signaling followed by STAT3 activation downregulated both *crx* and Rhodopsin expression. We used conditional knock-out mice devoid of STAT3 activation in the retina and a method of introducing exogenous genes by electroporation that allowed dominant-negative form of STAT3 (STAT3F) to be efficiently expressed in the retinal explants derived from P0 mice (P0 retinal explants), while maintaining the original tissue structure of neural retina. We also demonstrated that STAT3 activation was rapidly downregulated, when presumptive rod photoreceptor cells began to express Rhodopsin and differentiate into rod photoreceptor cells in vivo in the postnatal period. The results showed that persistent activation of STAT3 was responsible for the CNTF-induced inhibition of both *crx* and Rhodopsin expression in the P0 retinal explants. Next, we investigated whether precocious rod photoreceptor cell differentiation occurs before P0 in STAT3-deficient retina. We found neither significant difference in timing of Rhodopsin expression nor upregulation of *crx* expression overall, although we occasionally found a precocious upregulation of *crx* mRNA in STAT3-deficient retinas.

Thus, downregulation of STAT3 activation is required for presumptive rod photoreceptor cells to differentiate in postnatal retina and may contribute as one of the regulatory factors to determine the time of onset of rod photoreceptor cell differentiation. It is likely that several other independent pathways are necessary for proper temporal rod photoreceptor cell differentiation.

Results

Rhodopsin expression in the ONL of P0 retinal explants was inhibited by CNTF

First, we analyzed the effect of CNTF on Rhodopsin expression in P0 retinal explants, in which retinal cells followed developmental processes closely resembling those in vivo (Tomita et al., 1996) (Figs. 1Aa, b, m). Consistent with previous reports (Belliveau et al., 2000; Ezzeddine et al., 1997; Kirsch et al., 1998; Neophytou et al., 1997; Schulz-Key et al., 2002), strong inhibition of Rhodopsin expression in the ONL of P0 retinal explants was observed in the presence of CNTF (50–100 ng/ml) both at day 5 (Fig. 1Ac) and day 10 (data not shown).

The inhibition of Rhodopsin expression by CNTF was not definitive, and the retinal cells resumed expressing Rhodopsin when the CNTF was removed. Rhodopsin-expressing cells appeared in 2 days after removing CNTF following 3–5 days of exposure (Fig. 1Ad), and their expression increased to be observed in most of the cells in the ONL until the end (Fig. 1An). Moreover, the retinal cells in the ONL did not express any markers specific for other cell types examined, that is, HPC-1, PKC-α, and glutamine synthetase (markers for amacrine cells, bipolar cells, and Müller cells, respectively) after CNTF exposure (data not shown). These observations suggested that most presumptive rod photoreceptor cells remained undifferentiated rather than proceeding toward alternative cell fates. Although the possibility that the cells pursuing alternative cell fate in response to CNTF may have migrated from the ONL to other cell layers could not be completely ruled out, the number of such cells, if any, must have been small.

crx transcription in P0 retinal explants was also inhibited by CNTF

To clarify the inhibitory effect of CNTF on the processes leading to Rhodopsin expression, we examined expression pattern of *crx*, which is one of the key transcriptional activators of rod photoreceptor-specific genes including *rhodopsin* (Chen et al., 1997; Furukawa et al., 1997, 1999). *crx* expression is first observed in the outermost layer of the neural retina at E12.5 and spreads over entire ONL and outer half of the inner nuclear layer (INL) in the early postnatal period, eventually becoming restricted to the ONL in adult (Furukawa et al., 1997). The pattern of *crx* expression in retinal explants resembled the pattern in the retina in vivo (data not shown). In control P0 retinal explants at day 5, *crx* expression was observed throughout the entire ONL and outer half of the INL (Fig. 1Ao). After CNTF exposure, however, *crx* expression decreased dramatically in an in situ hybridization experiment performed in parallel (Fig. 1Ap), indicating that downregulation of *crx* expression might contribute to the inhibition of Rhodopsin expression. We further confirmed the downregulation of *crx* expression induced by addition of CNTF using semiquantitative analysis by real-time RT-PCR. After exposure to CNTF for 5 days, the relative level of *crx* mRNA expression in the P0 retinal explants was statistically downregulated to 38.6% (1.0 ± 0.043:0.386 ± 0.032, $P < 0.01$) (Fig. 1B).

STAT3 activation induced by CNTF was closely associated with inhibition of Rhodopsin expression in the ONL cells of P0 retinal explants

To elucidate the molecular mechanism underlying the CNTF-induced inhibition of Rhodopsin expression, we attempted to determine which of the downstream pathways of CNTF/gp130 signaling, the STAT3-mediated pathway or the SHP2-mediated pathway, was responsible for the downregulation of Rhodopsin expression. Following activation of the CNTF/gp130 receptor, STAT3 associates with several tyrosine residues in the gp130 receptor is phosphorylated and forms dimmers, then translocate to the nucleus where it activate the transcription of target genes (Akira, 1999; Takeda and Akira, 2000), whereas SHP2 (protein tyrosine phosphatase 2) associates with another tyrosine residue in the gp130 receptor and activates the RAS/MAPK pathway and/or the PI3 kinase pathway (Hirano et al., 1997; Ohtani et al., 2000).

First, we investigated STAT3 activation by immunohistochemical staining with anti-phosphoSTAT3 antibody. After 5 days of CNTF exposure, phosphorylated STAT3 staining was significantly observed in the nuclei of most ONL cells demonstrating that STAT3 signaling was indeed activated (Fig. 1Ag), but no such staining was seen in onbl cells at day 0 (Fig. 1Ae) nor in control ONL cells (Fig. 1Af). STAT3 activation in the ONL was then quantitatively investigated by immunoblot analysis (Fig. 1C). ONL cell lysates prepared from P0 retinal explants cultured for 5 days with or without exogeneous CNTF were analyzed with anti-STAT3 antibody that recognizes total STAT3 protein includ-

ing both phosphorylated and unphosphorylated STAT3 proteins, and anti-phosphoSTAT3 antibody that recognizes only phosphorylated STAT3 protein. The amount of total STAT3 protein and phosphorylated STAT3 protein increased 2-fold and 20-fold, respectively, after CNTF exposure. Thus, CNTF induced a 10-fold excess of phosphorylated endogenous STAT3 in ONL cells. We also confirmed the presence of CNTF receptor α in the ONL by immunoblot analysis (data not shown), which was in agreement with the previous reports (Kirsch et al., 1997; Schulz-Key et al., 2002).

Next, double immunostaining revealed a negative correlation between Rhodopsin and phosphorylated STAT3 expression (Figs. 1Ai–l). The cells of P0 retinal explants that failed to express Rhodopsin in the presence of CNTF were ONL cells, in which endogenous STAT3 is highly phosphorylated (Fig. 1Ak). Furthermore, a few phosphorylated STAT3 positive cells, found in the onbl of P0 retinal explants at day 0 (Fig. 1Ai) and in the ONL of P0 retinal explants cultured with CNTF only for the first 3 days followed by CNTF removal (Fig. 1Al), were devoid of Rhodopsin expression (Figs. 1Ai, l). Collectively, these findings demonstrated a negative correlation between STAT3 activation and Rhodopsin expression in P0 retinal explants. Under every condition examined, phosphoSTAT3 positive cells were also observed in the inner layer, where Rhodopsin expression does not occur, in consistent with the previous reports of CNTF receptor expression in retina (Kirsch et al., 1997; Schulz-Key et al., 2002).

STAT3 activation and Rhodopsin expression were negatively correlated in vivo

To determine that STAT3 activation and Rhodopsin expression are negatively correlated in the presumptive rod photoreceptor cells in vivo, we investigated their expression in the onbl at E18.5 and P0. STAT3 activation was observed in most of the cells in the presumptive rod photoreceptor cell layer, the onbl, at E18.5 (Fig. 2Ac), where no Rhodopsin expression was detected (Fig. 2Aa). On the contrary, STAT3 activation was barely seen in the onbl at P0 (Fig. 2Ad), the point in time when Rhodopsin-expressing cells first appeared (Fig. 2Ab). Phosphorylated STAT3 diminished markedly after birth, when Rhodopsin had just begun to be expressed in this layer. A low level of phosphorylated STAT3 remained in cells in the onbl at P0 that did not express rhodopsin (Fig. 2Ah, arrow). In both stages, abundant STAT3 activation was observed continuously in the inner layer (data not shown); however, these cells were unrelated to rhodopsin expression. The STAT3 activation in the onbl was downregulated earlier in the central retina than in the peripheral retina. Correspondingly, Rhodopsin expression started earlier in the central retina than in the peripheral retina. Thus, negative correlation between Rhodopsin expression and STAT3 activation was consistently observed during development of rod photoreceptor cells (Figs. 2Ag, h, high magnification and arrows). Immunoblot analysis further confirmed that the amount of total STAT3 protein and phosphorylated STAT3 protein in the onbl cells at E18.5 were 1.3-fold and 4.5-fold higher, respectively, than at P0 (Fig. 2B).

STAT3 activation, but not SHP2-mediated signaling, was required for CNTF to exert its inhibitory effect on Rhodopsin expression

Based on the above analysis, we hypothesized that the CNTF-induced inhibition of Rhodopsin expression was caused via STAT3 activation. To test this hypothesis, we investigated Rhodopsin expression in P0 retinal explants derived from STAT3 conditional knock-out mice in which STAT3 gene was disrupted only in the retina by using Cre-loxP system. Since STAT3 total knock-out mice could not be used because of embryonic lethality at a very early stage (Takeda et al., 1997), Cre-recombinase expression was directed under control of a retina-specific regulatory element of murine Pax6 (α-Cre) (Marquardt et al., 2001). Cre-recombinase activity was already detectable in E12.5 retina of α-Cre transgenic mice (Baumer et al., 2002; Marquardt et al., 2001). By generating double transgenic mice that carried both the α-Cre and CAG-CAT-GFP transgenes (Kawamoto et al., 2000), we confirmed that α-Cre-mediated recombination indeed occurred in most of the presumptive rod photoreceptor cells, that is, the onbl cells of the P0 retinas except for a few cells possibly due to the variegation of transgene expression (data not shown).

In the absence of exposure to CNTF, P0 retinal explants derived from $STAT3^{flox/-}$;α-Cre mice showed no obvious differences from those derived from their wild-type littermates, at day 0, 5, and 9. However, even after exposure to CNTF for 5 days (100 ng/ml), ONL cells of P0 retinal explants from $STAT3^{flox/-}$;α-Cre mice, in which virtually no phosphorylated STAT3 was detectable (Fig. 3Ac), exhibited Rhodopsin expression at day 5 (Fig. 3Aa); while P0 retinal explants from $STAT3^{flox/+}$ mice, littermates of the mutant mice considered to be phenotypically wild type, did not express Rhodopsin (Fig. 3Ab) with obvious STAT3 activation in the ONL after CNTF exposure (Fig. 3Ad). Furthermore, very small number

Fig. 1. Effects of CNTF on Rhodopsin expression and STAT3 activation in mouse P0 retinal explants. Retinal explants were prepared from P0 neural retina and immediately exposed to 100 ng/ml CNTF at day 0. (A) Double labeling with anti-Rhodopsin antibody and anti-phosphoSTAT3 antibody was performed at day 5, and examined with a confocal microscope. Rhodopsin expression (a–d, m, n). At day 0, a low level of rhodopsin expression was detected in only a few cells in the onbl (a) Control; At day 5, Rhodopsin expression was observed in the ONL (b). At day 5, no Rhodopsin expression was observed after CNTF exposure (c). At day 5, Rhodopsin expression was detected 2 days after CNTF removal following 3 days of exposure to CNTF (d) Control; At day 10, the level of Rhodopsin expression was higher than in "b" (m). Rhodopsin expression had spread throughout the ONL 5 days after CNTF removal following exposure to CNTF for 5 days (n). Detection of phosphorylated STAT3 (e–h). The phosphorylated STAT3 immunoreaction was detected in the nucleus, which was identified by Hoechst staining (data not shown). At day 0, a low level of phosphorylated STAT3 expression was detected in the onbl (e) Control; At day 5, almost no phosphorylated STAT3 expression was observed in the ONL (f). At day 5, a higher level of phosphorylated STAT3 expression was observed in most ONL cells after exposure to CNTF (g). Phosphorylated STAT3 expression was observed in the ONL 2 days after CNTF removal following CNTF exposure for 3 days, but at a lower level than in "g" (h). Merge (i–l). Note that the rhodopsin-expressing cells (arrowheads) in i and l did not express phosphorylated STAT3 and vice versa (arrow). *crx* mRNA expression at day 5 (o, p) Control; A high level of *crx* mRNA was observed in the ONL and outer half of the INL (o). Expression of *crx* mRNA was markedly downregulated after CNTF exposure (p). onbl, outer neuroblastic layer; inbl, inner neuroblastic layer; ONL, outer nuclear layer; INL, inner nuclear layer. (B) Real-time RT-PCR. Relative level of *crx* mRNA expression was statistically downregulated to 38.6% (1.0 ± 0.043:0.386 ± 0.032, $P < 0.01$), after CNTF exposure for 5 days. (C) Immunoblot analysis. Cell extracts were prepared from ONL cells of P0 neural retinal explants cultured with or without CNTF at day 5. After CNTF exposure, the relative amounts of total STAT3 (including both phosphorylated and unphosphorylated STAT3) and phosphorylated STAT3 proteins, measured by NIH image, increased 2-fold and 20-fold, respectively. α-tubulin was used as an inner control.

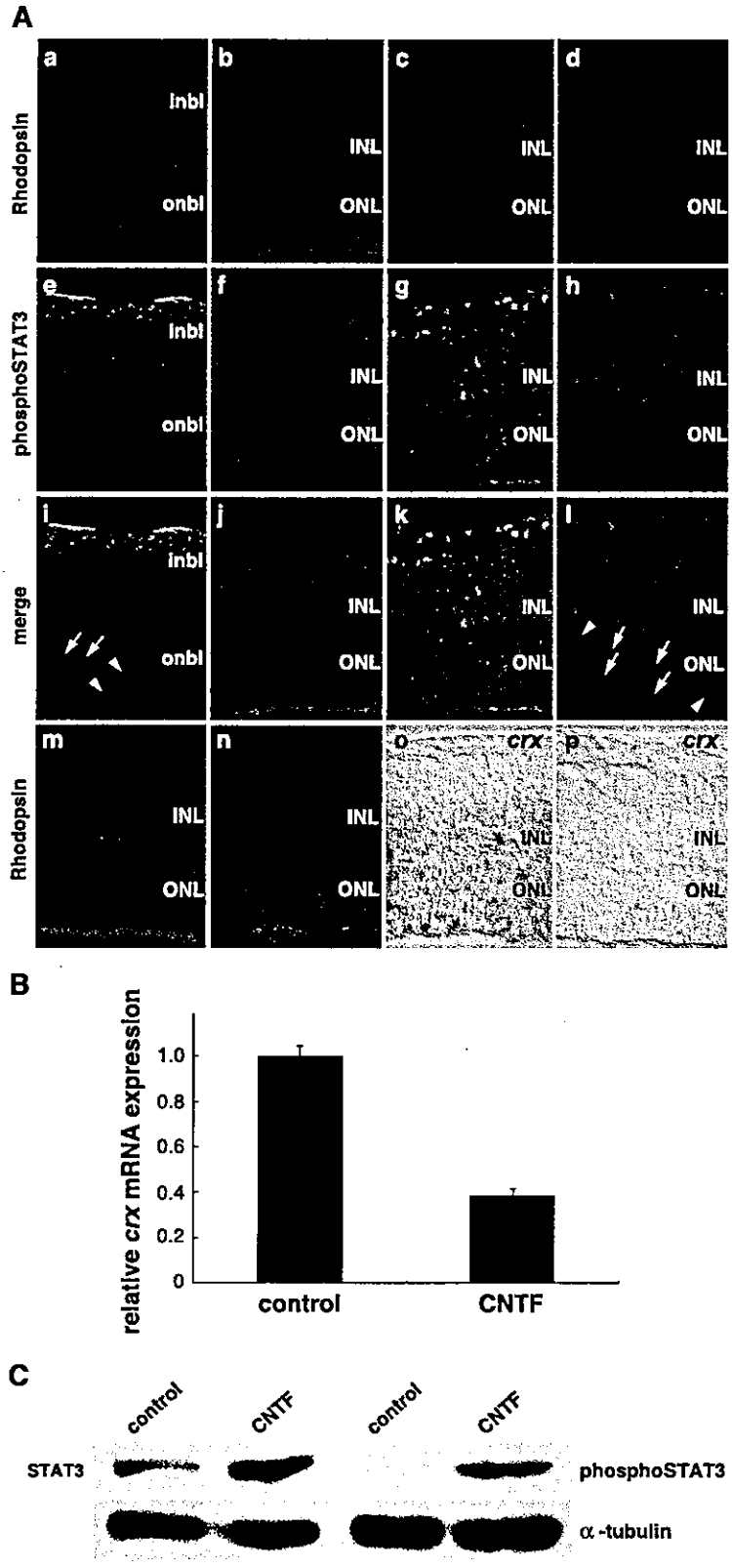
A
Rhodopsin
phosphoSTAT3
merge
Rhodopsin
a
b
c
d
e
f
g
h
i
j
k
l
m
n
o
p
inbl
onbl
INL
ONL
crx
B
relative crx mRNA expression
1.0
0.8
0.6
0.4
0.2
0
control
CNTF
C
control
CNTF
control
CNTF
STAT3
phosphoSTAT3
α-tubulin

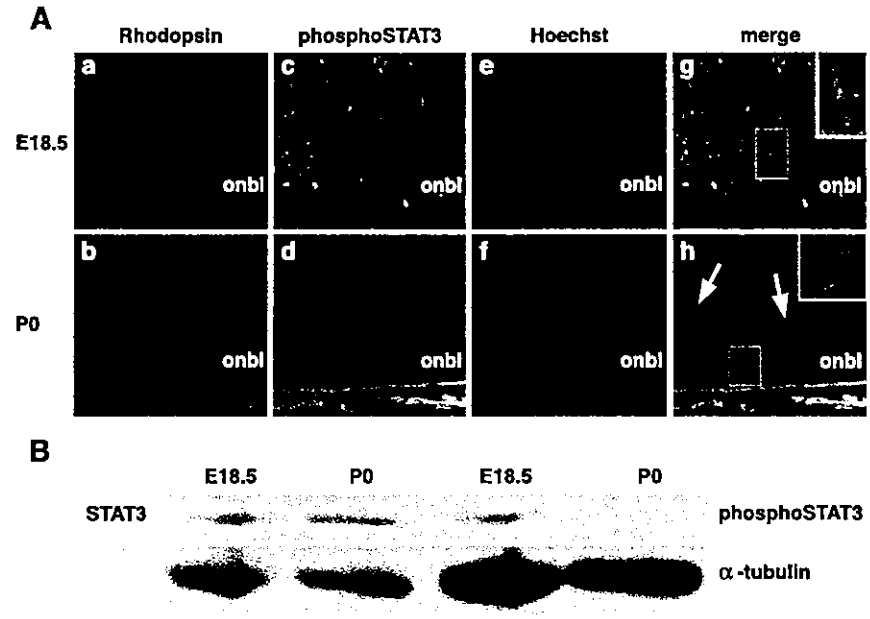

Fig. 2. Rhodopsin expression and STAT3 activation in E18.5 and P0 retina in vivo. (A) At E18.5, no Rhodopsin expression was detected in the onbl (a), whereas a high level of STAT3 activation was observed in the onbl (c). By contrast, at P0, a low level of Rhodopsin expression appeared in the onbl (b), whereas STAT3 activation had diminished markedly in the onbl (d). Phosphorylated STAT3 immunostaining was observed in nuclei (e, f). Merge; STAT3 activation and Rhodopsin expression are negatively correlated (g, h). Insets in g and h: Marked areas are magnified and merged in Hoechst staining images. Rhodopsin was negative in STAT3 activated cells, based on the phosphorylated STAT3 immunoreaction in the nucleus detected by Hoechst staining (inset of g). Rhodopsin-expressing cells showed no STAT3 activation (inset of h). Cells with a low level of phosphorylated STAT3 remaining showed no Rhodopsin expression (h, arrow). onbl, outer neuroblastic layer; inbl, inner neuroblastic layer; ONL, outer nuclear layer; INL, inner nuclear layer; Hoechst staining, blue. (B) Immunoblot analysis. Cell extracts were prepared from onbl cells at E18.5 and P0. Total STAT3 protein and phosphorylated STAT3 protein, measured by NIH image, were 1.3-fold and 4.5-fold higher, respectively, in onbl cells at E18.5 than at P0.

of phosphorylated STAT3 positive cells, which were occasionally found in the ONL probably due to discontinuity of transgene expression as described above, never expressed Rhodopsin with CNTF exposure (Fig. 3Ae). This indicated that only STAT3-deficient cells in the ONL escaped the inhibitory effect of CNTF on Rhodopsin expression.

We also investigated whether STAT3 activation was required for the inhibitory effect of CNTF on *crx* transcription. When cultured in the absence of CNTF, the ONL cells and outer half of the INL cells of P0 retinal explants from both $STAT3^{flox/-}$;α-Cre mice and $STAT3^{flox/+}$ mice expressed comparable levels of *crx* mRNA (Figs. 3Bn, p). Even after CNTF exposure, P0 retinal explants derived from $STAT3^{flox/-}$;α-Cre mice still clearly expressed *crx* mRNA in both the ONL and outer half of the INL (Fig. 3Bm), although at slightly lower level than P0 retinal explants derived from $STAT3^{flox/-}$;α-Cre mice cultured without CNTF. By contrast, retinal cells from $STAT3^{flox/+}$ mice expressed much less *crx* mRNA after CNTF exposure (Fig. 3Bo). This in situ hybridization experiment was performed in parallel. NIH image showed that the relative levels of *crx* mRNA expression after CNTF exposure to the levels of each control were 50% and 15% in $STAT3^{flox/-}$;α-Cre retina and $STAT3^{flox/+}$ retina, respectively. It is true, however, that *crx* mRNA was slightly downregulated by CNTF even in P0 retinal explants from STAT3 conditional knock-out mice, as compared with P0 retinal explants cultured without CNTF. It is possible that an indirect effect of earlier STAT3 gene disruption, for example, STAT family genes, other than STAT3 might have compensated for the loss of STAT3 function and reduced the mRNA level of *crx* instead of STAT3. These results indicated that the differences in expression of *crx* and Rhodopsin were attributable to the difference in STAT3 activation. After CNTF exposure, high level of *crx* expression and Rhodopsin expression were observed only in the absence of STAT3 activation.

To pursue the possibility that the other main pathway of CNTF/gp130 signaling, SHP2-mediated signal, might contribute to the inhibitory effect of CNTF on expression of *crx* and Rhodopsin, we prepared P0 retinal explants from $gp130^{F759}$ knock-in mice homozygotes, in which SHP2 activation was specifically blocked by the Tyr-759 mutation in the gp130 receptor without interfering with STAT3 activation (Ohtani et al., 2000). P0 retinal explants were cultured with CNTF (100 ng/ml) for 5 days. The same as their wild-type littermates, they never expressed Rhodopsin and expressed STAT3 activation obviously in ONL (Figs. 3Ag–l) as predicted. P0 retinal explants derived from $gp130^{F759/F759}$ knock-in mice, as well as those derived from their wild-type littermates, expressed a high level of *crx* in the absence of CNTF (Figs. 3Br, t), and exhibited markedly downregulated *crx* expression when exposed to CNTF (Figs. 3Bq, s). Semiquantification by NIH image showed that CNTF exposure induced downregulation of *crx* mRNA in $gp130^{F759/F759}$ knock-in retina as well as in wild-type retina (the relative levels of *crx* mRNA expression after CNTF exposure to the levels of each control were 5% and 13% in $gp130^{F759/F759}$ knock-in retina and wild-type retina, respectively). Thus, these findings indicated that SHP2 activation is not responsible for the effect of CNTF on Rhodopsin expression.

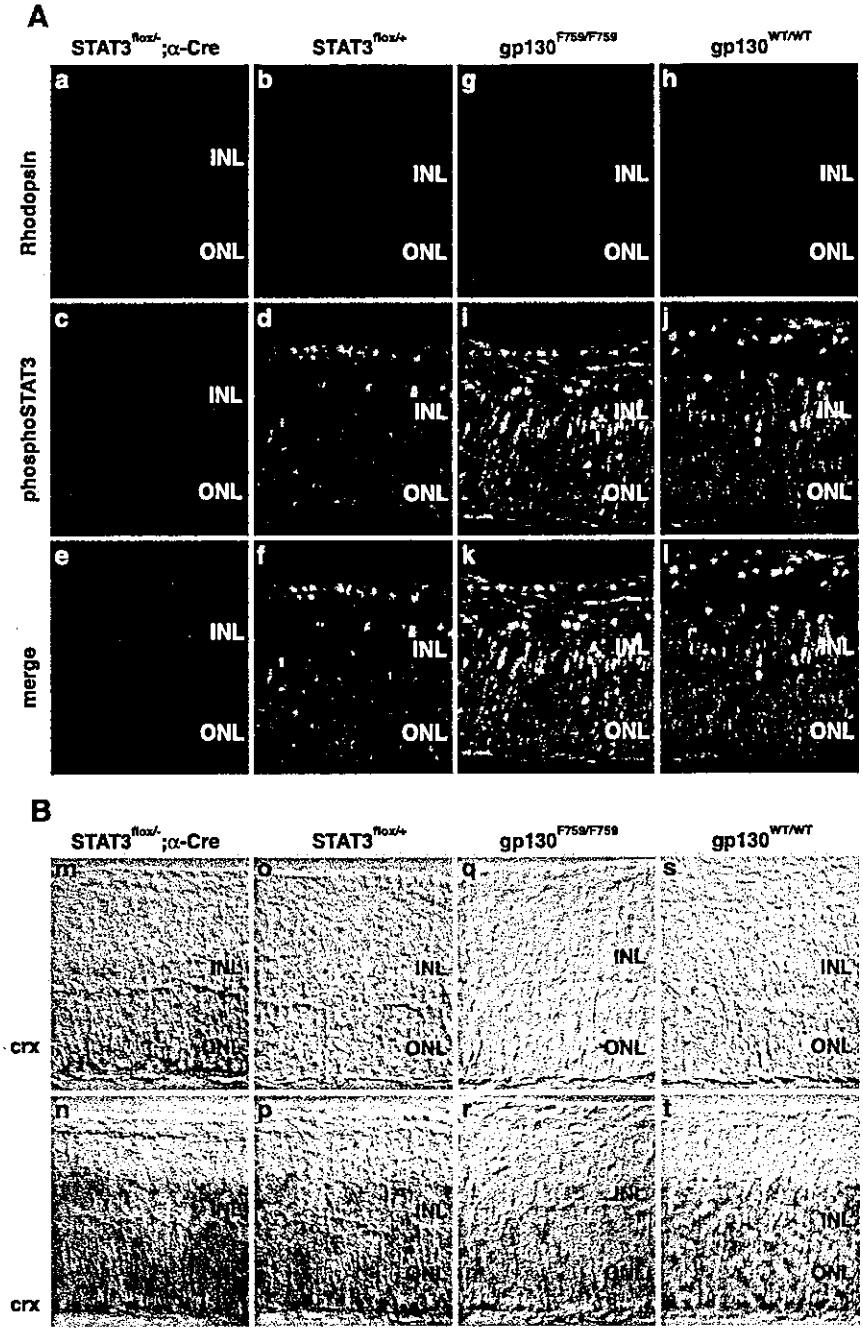

Fig. 3. Effects of CNTF on P0 retinal explants derived from CNTF/gp130 signal-deficient mice. All retinal explants were started at P0 and fixed at day 5. (A) All P0 retinal explants were cultured with CNTF. P0 retinal explants from STAT3$^{flox/-}$;α-Cre mice expressed Rhodopsin (a) and showed no STAT3 activation in most ONL cells (c). A small number of phosphoSTAT3 positive cells were occasionally seen in the ONL, but they never expressed Rhodopsin (e). By contrast, explants from STAT3$^{flox/+}$ mice, littermates of the mutant mice considered to be wild type, expressed no Rhodopsin (b) and showed STAT3 activation in the ONL (d). Merge (e, f). No STAT3 activation was detected in Rhodopsin-expressing cells. P0 retinal explants from gp130$^{F759/F759}$ mice with deficiency of SHP2 activation expressed no Rhodopsin (g) and showed STAT3 activation in the ONL (i), like P0 retinal explants prepared from wild-type littermates (h, j). Merge (k, l). (B) *crx* mRNA was highly expressed in the ONL and outer half of the INL of control P0 retinal explants (n, p, r, t). After CNTF exposure, P0 retinal explants from STAT3$^{flox/-}$;α-Cre mice clearly expressed *crx* mRNA (m), in contrast to P0 retinal explants from STAT3$^{flox/+}$ mice (o). CNTF actually decreased the *crx* mRNA expression level slightly in STAT3$^{flox/-}$;α-Cre retina, but the degree of the reduction was much smaller than that in STAT3$^{flox/+}$ retina. The relative levels of *crx* mRNA expression after CNTF exposure to the levels of each control measured by NIH image were 50% and 15% in STAT3$^{flox/-}$;α-Cre retina and STAT3$^{flox/+}$ retina, respectively. *crx* mRNA expression in P0 retinal explants from gp130$^{F759/F759}$ mice (q) and from wild-type littermates (s) were markedly reduced after CNTF exposure. The relative levels of *crx* mRNA expression to the levels of each control measured by NIH image were 5% and 13% in gp130$^{F759/F759}$ knock-in retina and wild-type retina, respectively. ONL, outer nuclear layer; INL, inner nuclear layer.

We also directly investigated whether MAPK activation is required for the inhibition by CNTF in wild-type animals by using PD098059 (Alessi et al., 1995), a specific inhibitor of MEK which is an activator of MAPK. Under standard condition in which MAPK was not activated in the presence of PD098059 (50 μM), P0 retinal explants never expressed Rhodopsin after exposure to CNTF (data not shown), further confirming that SHP2-mediated RAS/MAPK pathway is not involved in the CNTF-induced inhibition of rhodopsin expression in the postnatal retinal cells.

Blockade of STAT3-mediated signaling after starting P0 retinal explants was sufficient to override the CNTF-induced inhibitory effect on Rhodopsin expression

To exclude indirect effects of STAT3 deficiency in earlier embryonic period, we developed an efficient gene transfer system into cells in retinal explants by electroporation to attempt to block STAT3 activation only after starting retinal explants. Using this system, we introduced a dominant-negative form of STAT3 (STAT3F) at various times during development. STAT3F has a point mutation in the putative phosphorylation site, Tyr705, and it binds to the gp130 receptor, which in turn leads to competitively inhibited phosphorylation of endogenous STAT3 upon activation of the gp130 receptor (Minami et al., 1996; Nakajima et al., 1996). STAT3F gene fused with HA-tag was placed under control of the chicken beta-actin-cytomegalovirus hybrid promoter (CAG) (Niwa et al., 1991) that allows the transgenes to be expressed in all three layers including the ONL. We performed electroporation of plasmid CAG-HA-STAT3F with pCAG-EGFP, or plasmid CAG with pCAG-EGFP into the wild-type P0 retinal explants. The explants prepared from wild-type P0 retina were immediately subjected to electroporation of these constructs and then exposed to CNTF (50 ng/ml). At day 1, green fluorescence elicited by EGFP was already detected under a dissecting fluorescence microscope. Since the STAT3F gene was regulated under the same promoter, we assumed that expression of STAT3F had already started by day 1. The intensity of the green fluorescence increased for the first several days until it reached the peak level at around day 7, after which it persisted until at least day 10. We fixed the explants at day 7 and examined frozen sections of them. The cells into which STAT3F had been successfully introduced by electroporation were recognized by either green fluorescence or anti-HA immunostaining, and they were widely distributed throughout all three layers in the retinal explant (Fig. 4Aa). HA-tag fused with STAT3F was mainly in the cytoplasm, which is consistent with the fact that unphosphorylated STAT3 cannot be translocated into the nucleus (Takeda and Akira, 2000). After electroporation of plasmid CAG-HA-STAT3F with pCAG-EGFP, Rhodopsin-expressing cells were found even in the presence of CNTF (Fig. 4Ab). Notably, all the Rhodopsin-expressing cells were included in the cells that expressed dominant-negative form of STAT3 as identified by HA immunostaining, and all of them were in the ONL (Fig. 4Ac). None of the cells expressing control GFP vector alone, detected by green fluorescence of GFP (Fig. 4Ad), ever expressed Rhodopsin when the explants were cultured with CNTF (Fig. 4Ae). The *crx* mRNA expression after CNTF exposure was statistically higher in the pCAG-STAT3F-electroporated P0 retinal explants than in the control pCAG-electroporated P0 retinal explants, according to the results of real-time RT-PCR analysis with normalization to *gfp* mRNA, which was the transcript from the cotransfected plasmid CAG-EGFP (1.65 ± 0.05:1.0 ± 0.09, $P < 0.05$, Fig. 4B).

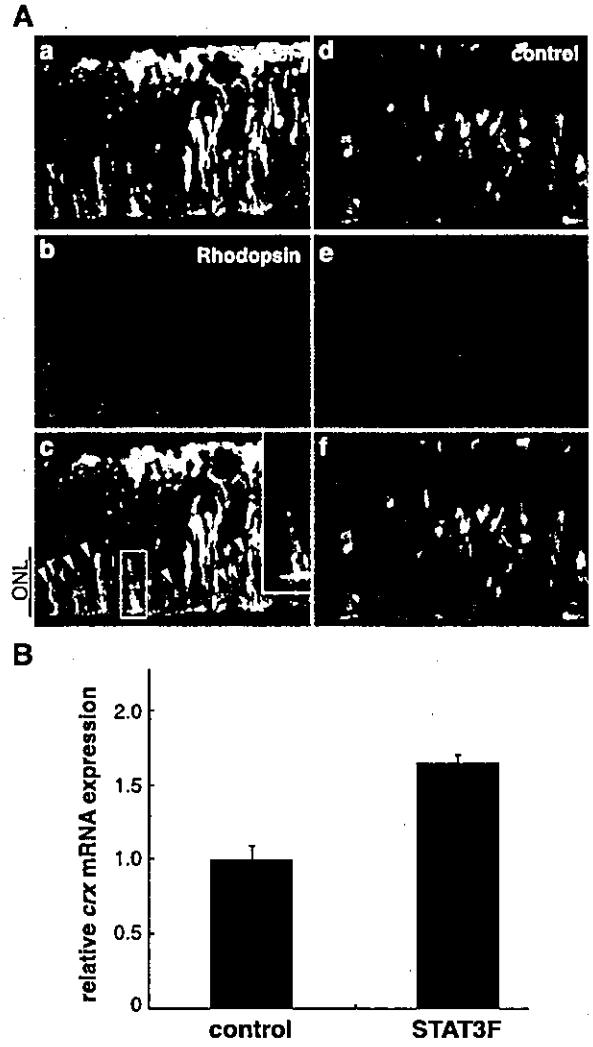

Fig. 4. Effect of CNTF in cells transfected with the dominant-negative form of STAT3 (STAT3F). (A) Wild-type retinal explants were started at P0, then electroporated and exposed to CNTF (50 ng/ml) for 7 days. STAT3F transfected cells were identified by HA immunostaining (a). Despite CNTF exposure, rhodopsin-expressing cells were observed only in the ONL (b), and they were all included in anti-HA immunopositive cells (merge, c). Inset in c: Marked area is magnified. Control vector was detected by green fluorescence protein (d), and no rhodopsin expression was seen when explants were cultured with CNTF (e, f). ONL, outer nuclear layer. (B) Real-time RT-PCR. Relative level of *crx* mRNA expression after CNTF exposure was statistically higher in cells from pCAG-STAT3F-electroporated P0 retinal explants than from control pCAG-electroporated P0 retinal explants with normalization to *gfp* mRNA, the transcript from the cotransfected plasmid CAG-EGFP (1.65 ± 0.05:1.0 ± 0.09, $P < 0.05$).

No significant effect of electroporation itself, such as cell death, abnormal retinal layer formation, or abnormal expression of differentiation markers, was observed under the present condition. Electroporated explants cultured without CNTF expressed Rhodopsin the same as untreated retinal explants (data not shown).

Thus, blockade of STAT3-mediated signaling after starting retinal explants derived from P0 mice (P0 retinal explants) was

sufficient to override the CNTF-induced inhibitory effect on Rhodopsin expression.

Furthermore, this inhibitory effect of CNTF, which was mediated by STAT3 activation, appeared to be cell-autonomous in the neural retina, since inhibition of Rhodopsin expression was overridden only in the cells in which dominant-negative form of STAT3 (STAT3F) was introduced.

Forced downregulation of STAT3 activation in the late embryonic retina was not sufficient for precocious rod photoreceptor cell differentiation

We have shown that persistent STAT3 activation by addition of CNTF in retinal explants derived from P0 mice inhibits Rhodopsin expression in vitro, and that downregulation of STAT3 activation precedes the onset of Rhodopsin expression in vivo, indicating that downregulation of STAT3 activation is required for Rhodopsin expression. We therefore investigated whether the forced downregulation of STAT3 activation in the late embryonic period induces precocious rod photoreceptor cell differentiation. If STAT3 activation is the only factor to determine the timing of rod photoreceptor cell differentiation, *crx* mRNA upregulation and Rhodopsin expression would be observed precociously in the STAT3-deficient retina. No precocious indications of Rhodopsin expression were observed, but the semiquantification analysis of *crx* mRNA expression showed some changes as described below.

Real-time RT-PCR analysis showed modest precocious upregulation of *crx* mRNA expression at E18.5 in STAT3$^{flox/-}$;α-Cre retina as compared with STAT3$^{flox/+}$ retina (1.6 ± 0.22 SE:1.0 ± 0.09 SE, $P = 0.03$, Fig. 5). The change was moderate in the mutant mice as a whole. This can be interpreted that the contribution of the STAT3 activation to inhibiting premature upregulation of *crx* mRNA is partial and some other factors may contribute in combination with STAT3 activation in vivo. In fact, we found that 25% of the individual STAT3$^{flox/-}$;α-Cre mice expressed an especially high level of *crx* mRNA, whereas the other expressed a normal (37.5%) to moderately high (37.5%) level, suggesting the presence of an alteration but with low penetrance. This suggested that there may be genetic redundancies that also affect *crx* mRNA expression.

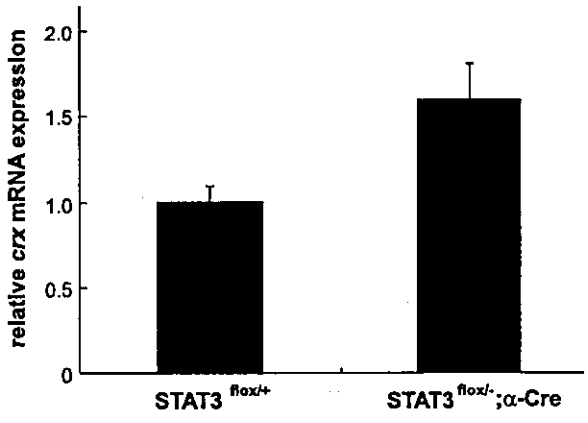

Fig. 5. Relative level of *crx* mRNA expression in STAT3-deficient retinas at E18.5. Real-time RT-PCR showed modest precocious upregulation of *crx* mRNA expression in the STAT3-deficient mice (STAT3$^{flox/-}$;α-Cre: STAT3$^{flox/+}$; 1.6 ± 0.22 SE:1.0 ± 0.09 SE, $P = 0.03$, $n = 8:6$).

There was no significant difference between STAT3$^{flox/-}$;α-Cre mice and STAT3$^{flox/+}$ mice in the numbers of the Rhodopsin-expressing cells, possibly because the time of onset of Rhodopsin expression is not determined solely by the downregulation of STAT3 activation.

We also tried to downregulate STAT3 activation in the embryonic retina in vitro by introducing STAT3F into wild-type retinal explants derived from E15 to E17 mice using electroporation. This method could rule out the possibility that the phenotypes described above are the results of indirect effects of STAT3 deficiency at some period before the birth of presumptive rod photoreceptor cells. When we examined retinal explants on the day corresponding to E18, that is, the day before initial expression of Rhodopsin in the control explants, and to P0, we found no precocious Rhodopsin positive cells in the retinal explants (data not shown), and identified Rhodopsin expression later, the same as in the unelectroporated retinal explants. This indicated that earlier blockade of STAT3 activation was insufficient to cause premature expression of Rhodopsin.

Discussion

Presumptive rod photoreceptor cells in outer half of the neural retina first appeared to be postmitotic in the late embryonic period (Cepko et al., 1996; Young, 1985) and start to express one of the terminal differentiation markers, Rhodopsin, in the early postnatal period. This interval between the final cell cycle and the onset of Rhodopsin expression is known to be several days (Morrow et al., 1998a,b). It has been postulated that both accumulation of cell intrinsic factors to promote differentiation and release from inhibitory extracellular signaling included in the embryonic retina might be important in determining the onset of Rhodopsin expression in the early postnatal period (Kirsch et al., 1998; Levine et al., 2000; Neophytou et al., 1997; Schulz-Key et al., 2002). Here we focus on the fact that CNTF that is present in the embryonic retina and downregulated in the postnatal retina inhibits Rhodopsin expression (Ezzeddine et al., 1997; Kirsch et al., 1998; Levine et al., 2000; Neophytou et al., 1997; Schulz-Key et al., 2002). We demonstrate that STAT3 activation mediates this inhibition, via one of the photoreceptor cell-specific gene activator, *crx*. Furthermore, we demonstrate that the negative correlation of Rhodopsin expression and STAT3 activation in perinatal retina and downregulation of STAT3 activation are required, although not sufficient, for presumptive rod photoreceptor cells to differentiate into rod photoreceptor cells.

CNTF downregulates expression of crx and Rhodopsin via STAT3 activation in P0 retinal explants

To analyze the mechanism of the CNTF-induced inhibition of Rhodopsin expression, we utilized the organ culture system of mouse neural retina started at P0, since this system maintains the microenvironmental condition surrounding the presumptive rod photoreceptor cells similar to that in vivo, in terms of cell density, cell distribution, and temporal expression profiles of various cell-type-specific markers of the retinal cells (Tomita et al., 1996), and it also allowed us to introduce exogenous genes of interest easily. We confirmed that CNTF exposure induces the inhibition of Rhodopsin expression while sustaining the competence for rod photoreceptor cells in P0 retinal explants.

In the present study, we showed that CNTF also downregulated homeobox gene *crx* dramatically. *crx* is one of the upstream transcription activators of *rhodopsin*, and rapid upregulation of *crx* expression is well correlated with the rapid increase in Rhodopsin expression as well as the expression of a series of photoreceptor-specific genes during normal retinal development (Chen et al., 1997; Furukawa et al., 1997, 1999, 2002; Livesey et al., 2000). Besides, expression of photoreceptor-specific genes including *rhodopsin* is greatly reduced in Crx knock-out mice (Furukawa et al., 1999). Thus, downregulation of the expression of photoreceptor-specific genes including *rhodopsin* by CNTF may occur through *crx* repression.

Then, which signal transduction pathway downstream from CNTF inhibited the expression of *crx* and Rhodopsin? CNTF is one of cytokines that activates gp130 receptor together with leukemia inhibitory factor (LIF) receptor β. They in turn recruit signal transducing molecules, such as STAT3 and SHP2, through which CNTF-induced cytokine signaling diverges into multiple downstream pathways that regulate cell growth, differentiation, survival, and so on (Hirano et al., 1997; Ohtani et al., 2000). Although both the STAT3- and SHP2-mediated pathways may be potentially activated in onbl/ONL cells following exposure to CNTF, expression of *crx* and Rhodopsin was only inhibited in the cells in which STAT3 had been activated. In addition, when CNTF exposure was discontinued and STAT3 activation was downregulated, Rhodopsin expression resumed, raising the possibility that STAT3 activation may be the cause of inhibition of Rhodopsin expression.

To test this possibility, we attempted to separate signaling pathways, which are supposed to be activated by CNTF, by preparing mutant P0 retinal explants from STAT3 conditional knock-out mice or gp130 mutant mice that are unable to activate SHP2 and investigated the inhibitory effect of CNTF in each culture. Our results demonstrated that STAT3 activation, but not SHP2 activation, is required for the CNTF-induced inhibitory effect on expression of *crx* and Rhodopsin in the ONL of P0 retinal explants.

It is still possible that earlier disruption of STAT3 gene might indirectly contribute to the lack of inhibitory effect of CNTF on expression of *crx* and Rhodopsin in the P0 retinal explants, since α-Cre-mediated gene disruption of the STAT3 locus occurs in the mid-embryonic period in $STAT3^{flox/-}$;α-Cre mice. To assess this possibility, we introduced dominant-negative form of STAT3, STAT3F, into P0 retinal explants of wild-type postnatal neural retina to disrupt functional STAT3 only after starting P0 retinal explants. For this purpose, we developed electroporation system allowing direct introduction of exogenous genes of interest into cells regardless of their stage of their cell cycle, in contrast to the method of retroviral infection (Tomita et al., 1996). We are able to transfect any gene into the organ culture including both postmitotic cells as well as mitotic cells by this method (data not shown). Moreover, the scattered population of transfected cells is appropriate to examine the cell-autonomous effect after gene introduction. No significant harmful effect of electroporation itself was observed and electroporated explant cells survived well for 7–10 days, in the same way as non-electroporated retinal explant cells. Expression of the gene introduced was sustained for at least 10 days under the conditions in this study. This demonstrates that blockade of STAT3 activation in ONL cells only after starting retinal explants derived from P0 mice is sufficient to override the CNTF-induced inhibition of expression of *crx* and Rhodopsin in a cell-autonomous manner. Although STAT3F expressing cells identified by anti-HA-immunostaining were widely distributed throughout all retinal layers, Rhodopsin expression occurred only in the ONL, suggesting that the potential to differentiate into rod photoreceptor cells is already restricted to the cells in the ONL.

Thus, it is now clear that STAT3 activation, induced by CNTF, is responsible for inhibition of expression of *crx* and Rhodopsin in the retinal explants derived from P0 mice (P0 retinal explants).

Molecular mechanisms of CNTF-induced inhibition of expression of crx and Rhodopsin

Knowing that STAT3 activation is the main cause of CNTF-induced downregulation of expression of Rhodopsin and its upstream activator, *crx* expression, several molecular mechanisms can be considered to explain the STAT3-mediated inhibitory effect on their expression. *crx* is one of the transcription activators of *rhodopsin* and is suggested to elevate expression level through the positive feedback mechanism (Furukawa et al., 2002) as discussed below. Thus, it is more important to identify the mechanism of *crx* repression to explain the mechanisms of inhibition of Rhodopsin expression.

Active STAT3 may bind to the upstream cis element of the *crx* gene near the sequence necessary for its activation to interfere the efficient approach and/or function of positive regulators competitively. This type of repression mechanism has been proposed in olfactory receptor neurons, in which the LIF/gp130 signal plays critical roles in maturation (Moon et al., 2002). Moon et al. showed that active STAT3 directly binds in the proximal resion of the promoter of *olfactory marker protein* gene, near the binding sites of the tissue-specific transcription activators, and negatively regulated the transcription. Since there is indeed a STAT3 binding consensus sequence upstream of the *crx* transcription initiation site, an excess of active STAT3 might affect binding of Crx or some other specific activators in a similar mechanism.

Another possibility is that active STAT3 sequesters cofactors, such as CBP/p300, that are required to induce *crx* gene expression. Assuming that the amounts of these cofactors in a cell are limited, they may be recruited competitively among various kinds of transcription factors. It is known that activation of bHLH transcription factors limit the level of common cofactors, CBP/p300, and inhibit STAT3 activation in neuronal cells (Sun et al., 2001). If CBP/p300 may be required for Crx (Yanagi et al., 2000) and bHLH gene products that may activate *crx* and/or *rhodopsin* genes (Ahmad, 1995), lack of CBP/p300, after excess of active STAT3 recruited CBP/p300 dominantly, might affect *crx* and/or *rhodopsin* gene expression.

It must be considered that there is a possibility that CNTF downregulates other transcription activators that upregulate Rhodopsin expression, whether functioning with Crx or not (Kimura et al., 2000; Mitton et al., 2000). For example, the transcription factor, neural retina leucine zipper (Nrl), has been shown to be one of the molecules essential for expression of *rhodopsin* and several other rod photoreceptor-specific genes based on the analyses of Nrl knock-out mice (Mears et al., 2001). There are still possibilities that STAT3 represses *rhodopsin* promoter directly or indirectly other than through repression of *crx*.

The effect of STAT3 on transcription of *crx* and *rhodopsin* may be regulated at multiple levels.

What determines the timing of the differentiation of postmitotic retinal cells in the ONL into rod photoreceptor cells?

As discussed above, presumptive rod photoreceptor cells in the ONL that exited cell cycle in the late embryonic period are kept undifferentiated until they rapidly upregulate *crx* expression and start to express the terminal differentiation marker Rhodopsin in the early postnatal period. How is this process precisely controlled? Obviously, both positive and negative factors may be involved (Kageyama and Nakanishi, 1997). Regarding negative factors, we propose STAT3 activation by CNTF that prevents presumptive rod photoreceptor cells from differentiation, based on the negative correlation between STAT3 activation and Rhodopsin expression during retinal development in vivo, and the results of persistent STAT3 activation in vitro; STAT3 was highly activated in presumptive rod photoreceptor cells at E18.5, and was rapidly inactivated to below the level of detection at P0, which corresponded to the onset of rapid upregulation of *crx* and Rhodopsin expression (Fig. 6Aa). If persistent STAT3 activation occurs in presumptive rod photoreceptor cells in P0 retinal explants, neither *crx* nor Rhodopsin can be upregulated (Fig. 6Ab). Active STAT3 allows the presumptive rod photoreceptor cells to retain their competence to differentiate into rod photoreceptor cells, and differentiation can be restarted as long as the inhibitory extrinsic cue is eliminated (Figs. 1Ab, d, m, n, and 4b), which is consistent with the estimated function in vivo.

Then, is downregulation of STAT3 activation sufficient to trigger Rhodopsin expression? To answer this question, we investigated whether conditional disruption of STAT3 in the late embryonic period leads to precocious differentiation of rod photoreceptor cells. If STAT3 activation were the only factor to determine the time of onset, Rhodopsin expression would start before P0 in STAT3-deficient mice. However, that did not happen at significant level. But semiquantitative analysis by real-time RT-PCR showed that 25% of the individual mutant retinas exhibited precocious upregulation of *crx* mRNA, suggesting that downregulation of STAT3 activation has at least some roles in determining the time of onset of rod photoreceptor cell differentiation. This change was moderate in the mutants as a whole, but obvious in 25% of the individual mutant embryonic retinas. The low penetrant change often indicates genetic redundancies; therefore, some other factors besides downregulation of STAT3 activation may be necessary to determine the time of onset of upregulation of *crx* mRNA. This is why we consider that downregulation of STAT3 activation might contribute to determin-

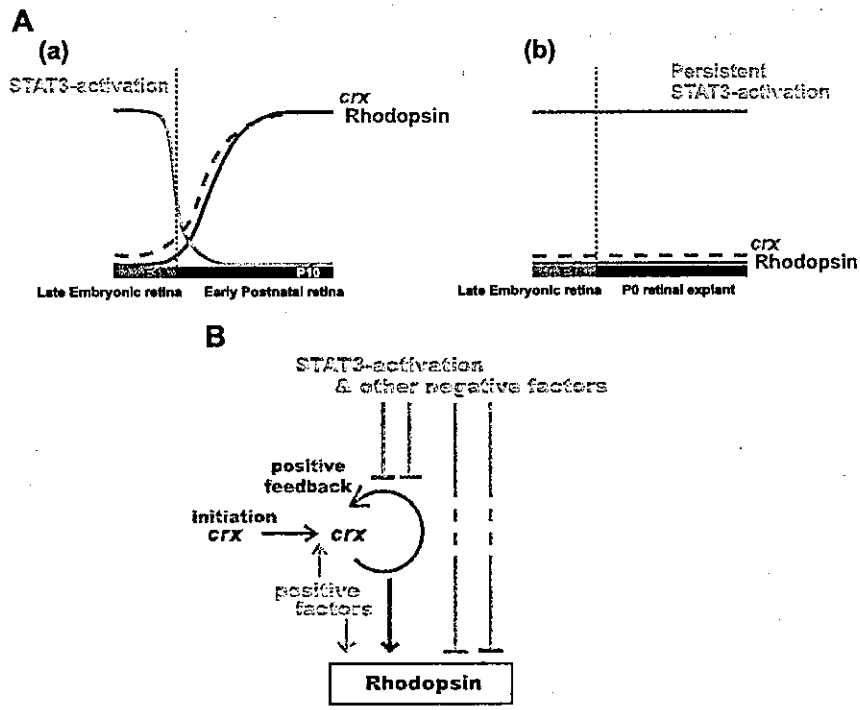

Fig. 6. (A) Molecular mechanisms regulating rod photoreceptor cell differentiation in perinatal retina. Rod photoreceptor cells differentiate in the outer layer of the neural retina. STAT3 is highly activated in this layer of the late embryonic retina in vivo, but its activation is rapidly downregulated in the early postnatal retina. This allows upregulation of *crx* transcription, which in turn contributes to upregulation of expression of Rhodopsin, one of the terminal differentiation markers, in the early postnatal retina (a). Persistent STAT3 activation in this layer of P0 retinal explants prevents upregulation of *crx* transcription and Rhodopsin expression in a cell-autonomous manner (b). (B) A model for STAT3 activation as one of the potential negative regulators of *crx* and Rhodopsin expression based on our results of STAT3-deficient mice and stage-specific disruption of STAT3 activation after introducing the dominant-negative STAT3 (STAT3F). We propose a model in which STAT3 activation inhibits a high level of *crx* expression that is upregulated possibly via a positive feedback mechanism. Several other factors, including positive and/or negative factors, would contribute together. STAT3 activation inhibits Rhodopsin expression mainly through inhibition of a high level of *crx* expression and possibly through other pathways that are regulated by positive and/or negative factors. Thus, downregulation of STAT3 activation might contribute partially, although not definitively, to determining the time of onset of Rhodopsin expression in presumptive rod photoreceptor cells.

ing the time of onset of rod photoreceptor cell differentiation in the presumptive rod photoreceptor cells, although it is not a major contribution. This kind of low penetrant phenotype is also observed in a certain gene disrupted mice, such as Ring 1A-deficient mice that have an only low penetrant homeotic alteration in the axial skeleton associated with minor alterations of Hox gene expression (del Mar Lorente et al., 2000). Since Ring 1A functions only as one of the members of transcriptional repressors that negatively regulate Hox gene expression, other members of transcriptional repressors, such as Ring 1B, would compensate the function in Ring 1A-deficient mice.

Knowing that STAT3 activation is not absolutely crucial for the suppression of Rhodopsin expression in the embryonic period, we propose a possible influence of STAT3 activation on *crx* expression. It has been suggested that transcriptional regulation of *crx* is divided into two steps (Furukawa et al., 2002). In the first step, *crx* is initially expressed at a low level in the late embryonic period, and in the second step, rapid upregulation occurs possibly mediated via a positive feedback mechanism by Crx itself together with unknown factors (Furukawa et al., 2002). Based on our observations, the first step of this model begins despite continuous STAT3 activation, while the second step initiated in the early postnatal period after STAT3 activation has declined. Here we show that a high level of *crx* expression is inhibited by STAT3 activation induced by addition of CNTF in the P0 retinal explants, and this may be attributable to the inhibition of the second step (Fig. 6B). Taken together, the attractive model involves a low level of expression that is insensitive to the negative effect of STAT3 activation in the late embryonic period and a high level of expression that is sensitive to the negative effect of STAT3 activation in the early postnatal period. Lack of precocious expression of Rhodopsin even in the absence of STAT3 activation in the late embryonic period instead supports the notion that a combination of Crx and other factors, as yet unidentified, is required for the high level of *crx* expression that allows Rhodopsin expression in postmitotic retinal cells in the ONL. In addition, positive factors promoting Rhodopsin expression other than Crx and/or the suppression of certain negative factors other than the STAT3 activation would be necessary for the Rhodopsin expression and/or rod photoreceptor cell differentiation.

In conclusion, we propose here one of the potential regulatory mechanisms for rod photoreceptor cell differentiation in terms of expression of *crx* and Rhodopsin in the perinatal period. Downregulation of STAT3 activation is required in the postnatal period for proper rod photoreceptor cell differentiation. Furthermore, it is conceivable that downregulation of STAT3 activation contributes as one of the factors to determining the time of onset of rod photoreceptor cell differentiation, although further analyses are required to clarify other factors.

Experimental methods

Neural retinal explant culture

Retinal explant culture was performed using P0 mouse neural retina based on the protocol described by Tomita et al. (1996). Briefly, eyes were enucleated and neural retinas were isolated and placed on a Millicell chamber filter (Millipore: pore size: 0.4 μm) with the ganglion cell layer facing up. The chamber was then placed in a 6-well culture plate, containing 50% MEM (GIBCO), 25% HBSS (GIBCO), 25% horse serum (Thermo Trace), 200 mM L-glutamine, and 6.75 mg/ml D-glucose. Explants were incubated at 34°C in 5% CO_2. Medium was changed every 1–2 days.

A 10 μg/ml stock solution of recombinant rat CNTF (R&D) in MEM was maintained at −20°C. Once thawed, it was maintained at 4°C and used within 3 days. CNTF was used in concentrations of 50–100 ng/ml in this system, just enough to completely inhibit Rhodopsin expression in the ONL of P0 retinal explants, without causing any obvious changes in the three-layered structure of the retina, in the morphology of any of the cell types, or in expressions of molecular markers of cell types other than rod photoreceptor cells. These concentrations are somewhat higher than those used in previous studies (Ezzeddine et al., 1997; Kirsch et al., 1998; Schulz-Key et al., 2002), in part because the medium contained a relatively large amount of horse serum that may include antagonizing activity to CNTF, or because the membrane inserted between the explants and the medium affected our culture system.

Animals

ICR and C57B/6 mice were purchased from Clea Japan, INC. and the Charles River Laboratory.

STAT3 ^{flox} mice and STAT3$^{+/-}$ mice were generated by Dr. Akira's Lab (Sano et al., 1999; Takeda et al., 1997), and gp130^{F759} knock-in mice by Dr. Hirano's Lab (Ohtani et al., 2000). α-Cre transgenic mice, which express Cre-recombinase only in the retina, were generously provided by Dr. Gruss (Marquardt et al., 2001). The mice were used in conjunction with genotyping. CAG-CAT-EGFP transgenic mice, used to show the expression of Cre-recombinase, were kindly provided by Dr. Miyazaki (Kawamoto et al., 2000).

In the experiments on mutant mice, P0 retinal explant from one eye was exposed to CNTF and P0 retinal explants from the other eye was not exposed to CNTF to equalize the basal developmental stage.

Immunohistochemistry

Cryosections (12–14 μm) of retinal explants were fixed with 4% paraformaldehyde and prepared as described elsewhere (Tomita et al., 1996). Cryosections of E18.5 and P0 eyes (12 μm) were prepared by perfusing mice with 4% paraformaldehyde, enucleated, and post-fixed in 4% paraformaldehyde. Sections were first incubated with 0.1% Triton, 10% goat serum in PBS, and then at 4°C with primary antibodies to retinal cell-specific markers, that is, rabbit anti-Rhodopsin (1:2000 LSL), mouse anti-glutamine synthetase (1:400 Molecular Probe), mouse anti-HPC1 (1:600 Sigma), and mouse anti-PKCα (1:50 Molecular Probe), diluted in 0.1% Triton and 2% goat serum. Sections were then incubated with the secondary antibody, Alexa 568-conjugated goat anti-rabbit, or Alexa 488-conjugated goat anti-mouse IgG (1:500, Molecular Probe), respectively. For immunostaining of rabbit anti-phosphoSTAT3 (1:50 Cell Signaling) and rat anti-HA (1:500, Roche Diagnostics GmbH), sections were pre-incubated at 100°C for 5 min with tissue retrieval solution (TRS, Sigma #1699) and then placed on ice for 20 min. Next, they were incubated in 1% H_2O_2, in blocking agent, and then at 4°C overnight, with primary antibody diluted in blocking agent with 0.3% or 0.1% Triton, respectively. The sections were incubated with biotin-conjugated donkey anti-rabbit IgG (1:500 Chemicon) or biotin-conjugated goat anti-rat IgG (1:500, Vector), then with prepared avidin-biotin-peroxidase complex (Vector). Finally,

immunoreactions were detected with a tyramide signal amplification (TSA) fluorescein system (Perkin Elmer Life Science). Nuclei were stained with the nuclear dye bisbenzimide 1:1000 from a stock solution of 10 mg/ml Hoechst 33258 (Sigma). GFP fluorescence disappeared after TRS treatment. For double immunostaining, all processes were performed sequentially. To strip away the primary antibody, sections were incubated with 200 mM glycine (pH 2.2). The double immunostained sections were examined with a laser scanning confocal microscope (LSM510, Carl Zeiss).

Real-time RT-PCR

Total RNA was extracted from retina, and cDNAs were synthesized after RNase-free DNase (Invitrogen) treatment. Real-time PCR was performed using an ABI PRISM 7700, with SYBR green (Molecular Probe). The primers for *crx* detection have been described by Furukawa et al. (1999). The results are presented as ratios of mRNA expression normalized to an inner control gene: *β-actin* or *gfp* mRNA in electroporated cells.

Immunoblot analysis

Retinal cells from the outer layer were collected by cutting the neural retina horizontally, as described by Schulz-Key et al. (2002) with minor modification. Briefly, neural retinal explants and neural retinas were flat-mounted and cryosections were made at a 60-μm thickness from the ONL/onbl side. The extracts were electrophoretically transferred to membranes and incubated in rabbit anti-STAT3 (1:1000, Cell Signaling) or rabbit anti-phosphoSTAT3 (1:1000, Cell Signaling), with mouse anti-α-tubulin (1:2000, Sigma) to equalize the amount of protein in each sample, then with both horseradish peroxidase-conjugated anti-rabbit IgG and anti-mouse IgG. The specific proteins were detected with an ECL system (Pharmacia-Amersham).

Electroporation

DNA, 5 μg/μl in PBS(−), was loaded on the top of agarose gel placed on a plate-type electrode. After a retinal explant on the membrane had been placed on the DNA, a disk type electrode was used to apply electric pulses (20 V, 50 ms, 6 times) with the electroporator (CUY21 NEPPA GENE), without contacting the tissue. The retinal explant was then immediately replaced in the medium and incubated as described above. An expression vector carrying a cDNA encoding a dominant-negative form of STAT3F (Minami et al., 1996; Nakajima et al., 1996) under control of the CAG promoter (Niwa et al., 1991), pCAG-STAT3F, was cotransfected with pCAG-EGFP (an expression vector containing the enhanced green fluorescent protein [EGFP]) (10:1). Empty transfection vector, pCAG, with pCAG-EGFP was electroporated as a control.

In situ hybridization

In situ hybridization was performed on 12- to 14-μm-thick cryosections. The probe for *crx* (a generous gift from Dr. Furukawa) (Furukawa et al., 1997) was full-length and detected with a digoxigenin labeling system. To compare expression levels, these processes were simultaneously performed in parallel under the same conditions on the same glass.

Acknowledgments

We appreciate Dr. Peter Gruss for generously providing the α-Cre transgenic mice, Dr. Takahisa Furukawa for the *crx* cDNA, Dr. Jun-ichi Miyazaki for the CAG-CAT-EGFP transgenic mice, and Dr. Hitoshi Niwa for the plasmid CAG. We also thank Hironori Kawahara for preparing the illustrations. This work was supported by grants from the Ministry of Education, Science and Culture of Japan to H.O. and National Grant-in-Aid for the Establishment of High-Tech Research Center in a Private University.

References

Ahmad, I., 1995. Mash-1 is expressed during ROD photoreceptor differentiation and binds an E-box, E(opsin)-1 in the rat opsin gene. Brain Res., Dev. Brain Res. 90, 184–189.

Akira, S., 1999. Functional roles of STAT family proteins: lessons from knockout mice. Stem Cells 17, 138–146.

Alessi, D.R., Cuenda, A., Cohen, P., Dudley, D.T., Saltiel, A.R., 1995. PD 098059 is a specific inhibitor of the activation of mitogen-activated protein kinase kinase in vitro and in vivo. J. Biol. Chem. 270, 27489–27494.

Altshuler, D., Cepko, C., 1992. A temporally regulated, diffusible activity is required for rod photoreceptor development in vitro. Development 114, 947–957.

Altshuler, D., Lo Turco, J.J., Rush, J., Cepko, C., 1993. Taurine promotes the differentiation of a vertebrate retinal cell type in vitro. Development 119, 1317–1328.

Baumer, N., Marquardt, T., Stoykova, A., Ashery-Padan, R., Chowdhury, K., Gruss, P., 2002. Pax6 is required for establishing naso-temporal and dorsal characteristics of the optic vesicle. Development 129, 4535–4545.

Belliveau, M.J., Young, T.L., Cepko, C.L., 2000. Late retinal progenitor cells show intrinsic limitations in the production of cell types and the kinetics of opsin synthesis. J. Neurosci. 20, 2247–2254.

Cepko, C.L., Austin, C.P., Yang, X., Alexiades, M., Ezzeddine, D., 1996. Cell fate determination in the vertebrate retina. Proc. Natl. Acad. Sci. U. S. A. 93, 589–595.

Chen, S., Wang, Q.L., Nie, Z., Sun, H., Lennon, G., Copeland, N.G., Gilbert, D.J., Jenkins, N.A., Zack, D.J., 1997. Crx, a novel Otx-like paired-homeodomain protein, binds to and transactivates photoreceptor cell-specific genes. Neuron 19, 1017–1030.

del Mar Lorente, M., Marcos-Gutiérrez, C., Pérez, C., Schoorlemmer, J., Ramírez, A., Magin, T., Vidal, M., 2000. Loss- and gain-of-function mutations show a Polycomb group function for Ring1A in mice. Development 127, 5093–5100.

Edlund, T., Jessell, T.M., 1999. Progression from extrinsic to intrinsic signaling in cell fate specification: a view from the nervous system. Cell 96, 211–224.

Ezzeddine, Z.D., Yang, X., DeChiara, T., Yancopoulos, G., Cepko, C.L., 1997. Postmitotic cells fated to become rod photoreceptors can be respecified by CNTF treatment of the retina. Development 124, 1055–1067.

Furukawa, T., Morrow, E.M., Cepko, C.L., 1997. Crx, a novel otx-like homeobox gene, shows photoreceptor-specific expression and regulates photoreceptor differentiation. Cell 91, 531–541.

Furukawa, T., Morrow, E.M., Li, T., Davis, F.C., Cepko, C.L., 1999. Retinopathy and attenuated circadian entrainment in Crx-deficient mice. Nat. Genet. 23, 466–470.

Furukawa, A., Koike, C., Lippincott, P., Cepko, C.L., Furukawa, T., 2002. The mouse Crx 5′-upstream transgene sequence directs cell-specific and developmentally regulated expression in retinal photoreceptor cells. J. Neurosci. 22, 1640–1647.

Harris, W.A., 1997. Cellular diversification in the vertebrate retina. Curr. Opin. Genet. Dev. 7, 651–658.

Hirano, T., Nakajima, K., Hibi, M., 1997. Signaling mechanisms through gp130: a model of the cytokine system. Cytokine Growth Factor Rev. 8, 241–252.

Kageyama, R., Nakanishi, S., 1997. Helix-loop-helix factors in growth and differentiation of the vertebrate nervous system. Curr. Opin. Genet. Dev. 7, 659–665.

Kawamoto, S., Niwa, H., Tashiro, F., Sano, S., Kondoh, G., Takeda, J., Tabayashi, K., Miyazaki, J., 2000. A novel reporter mouse strain that expresses enhanced green fluorescent protein upon Cre-mediated recombination. FEBS Lett. 470, 263–268.

Kelley, M.W., Turner, J.K., Reh, T.A., 1994. Retinoic acid promotes differentiation of photoreceptors in vitro. Development 120, 2091–2102.

Kimura, A., Singh, D., Wawrousek, E.F., Kikuchi, M., Nakamura, M., Shinohara, T., 2000. Both PCE-1/RX and OTX/CRX interactions are necessary for photoreceptor-specific gene expression. J. Biol. Chem. 275, 1152–1160.

Kirsch, M., Lee, M.Y., Meyer, V., Wiese, A., Hofmann, H.D., 1997. Evidence for multiple, local functions of ciliary neurotrophic factor (CNTF) in retinal development: expression of CNTF and its receptors and in vitro effects on target cells. J. Neurochem. 68, 979–990.

Kirsch, M., Schulz-Key, S., Wiese, A., Fuhrmann, S., Hofmann, H., 1998. Ciliary neurotrophic factor blocks rod photoreceptor differentiation from postmitotic precursor cells in vitro. Cell Tissue Res. 291, 207–216.

Levine, E.M., Fuhrmann, S., Reh, T.A., 2000. Soluble factors and the development of rod photoreceptors. Cell. Mol. Life Sci. 57, 224–234.

Lillien, L., 1995. Changes in retinal cell fate induced by overexpression of EGF receptor. Nature 377, 158–162.

Livesey, F.J., Cepko, C.L., 2001. Vertebrate neural cell-fate determination: lessons from the retina. Nat. Rev., Neurosci. 2, 109–118.

Livesey, F.J., Furukawa, T., Steffen, M.A., Church, G.M., Cepko, C.L., 2000. Microarray analysis of the transcriptional network controlled by the photoreceptor homeobox gene Crx. Curr. Biol. 10, 301–310.

Marquardt, T., Ashery-Padan, R., Andrejewski, N., Scardigli, R., Guillemot, F., Gruss, P., 2001. Pax6 is required for the multipotent state of retinal progenitor cells. Cell 105, 43–55.

Mears, A.J., Kondo, M., Swain, P.K., Takada, Y., Bush, R.A., Saunders, T.L., Sieving, P.A., Swaroop, A., 2001. Nrl is required for rod photoreceptor development. Nat. Genet. 29, 447–452.

Minami, M., Inoue, M., Wei, S., Takeda, K., Matsumoto, M., Kishimoto, T., Akira, S., 1996. STAT3 activation is a critical step in gp130-mediated terminal differentiation and growth arrest of a myeloid cell line. Proc. Natl. Acad. Sci. U. S. A. 93, 3963–3966.

Mitton, K.P., Swain, P.K., Chen, S., Xu, S., Zack, D.J., Swaroop, A., 2000. The leucine zipper of NRL interacts with the CRX homeodomain. A possible mechanism of transcriptional synergy in rhodopsin regulation. J. Biol. Chem. 275, 29794–29799.

Moon, C., Yoo, J.Y., Matarazzo, V., Sung, Y.K., Kim, E.J., Ronnett, G.V., 2002. Leukemia inhibitory factor inhibits neuronal terminal differentiation through STAT3 activation. Proc. Natl. Acad. Sci. U. S. A. 99, 9015–9020.

Morrow, E.M., Belliveau, M.J., Cepko, C.L., 1998a. Two phases of rod photoreceptor differentiation during rat retinal development. J. Neurosci. 18, 3738–3748.

Morrow, E.M., Furukawa, T., Cepko, C.L., 1998b. Vertebrate photoreceptor cell development and disease. Trends Cell Biol. 8, 353–358.

Nakajima, K., Yamanaka, Y., Nakae, K., Kojima, H., Ichiba, M., Kiuchi, N., Kitaoka, T., Fukada, T., Hibi, M., Hirano, T., 1996. A central role for Stat3 in IL-6-induced regulation of growth and differentiation in M1 leukemia cells. EMBO J. 15, 3651–3658.

Neophytou, C., Vernallis, A.B., Smith, A., Raff, M.C., 1997. Muller-cell-derived leukaemia inhibitory factor arrests rod photoreceptor differentiation at a postmitotic pre-rod stage of development. Development 124, 2345–2354.

Niwa, H., Yamamura, K., Miyazaki, J., 1991. Efficient selection for high-expression transfectants with a novel eukaryotic vector. Gene 108, 193–199.

Ohtani, T., Ishihara, K., Atsumi, T., Nishida, K., Kaneko, Y., Miyata, T., Itoh, S., Narimatsu, M., Maeda, H., Fukada, T., et al., 2000. Dissection of signaling cascades through gp130 in vivo: reciprocal roles for STAT3- and SHP2-mediated signals in immune responses. Immunity 12, 95–105.

Sano, S., Itami, S., Takeda, K., Tarutani, M., Yamaguchi, Y., Miura, H., Yoshikawa, K., Akira, S., Takeda, J., 1999. Keratinocyte-specific ablation of Stat3 exhibits impaired skin remodeling, but does not affect skin morphogenesis. EMBO J. 18, 4657–4668.

Schulz-Key, S., Hofmann, H.D., Beisenherz-Huss, C., Barbisch, C., Kirsch, M., 2002. Ciliary neurotrophic factor as a transient negative regulator of rod development in rat retina. Invest. Ophthalmol. Visual Sci. 43, 3099–3108.

Sun, Y., Nadal-Vicens, M., Misono, S., Lin, M.Z., Zubiaga, A., Hua, X., Fan, G., Greenberg, M.E., 2001. Neurogenin promotes neurogenesis and inhibits glial differentiation by independent mechanisms. Cell 104, 365–376.

Takeda, K., Akira, S., 2000. STAT family of transcription factors in cytokine-mediated biological responses. Cytokine Growth Factor Rev. 11, 199–207.

Takeda, K., Noguchi, K., Shi, W., Tanaka, T., Matsumoto, M., Yoshida, N., Kishimoto, T., Akira, S., 1997. Targeted disruption of the mouse Stat3 gene leads to early embryonic lethality. Proc. Natl. Acad. Sci. U. S. A. 94, 3801–3804.

Tomita, K., Ishibashi, M., Nakahara, K., Ang, S.L., Nakanishi, S., Guillemot, F., Kageyama, R., 1996. Mammalian hairy and enhancer of split homolog 1 regulates differentiation of retinal neurons and is essential for eye morphogenesis. Neuron 16, 723–734.

Watanabe, T., Raff, M.C., 1990. Rod photoreceptor development in vitro: intrinsic properties of proliferating neuroepithelial cells change as development proceeds in the rat retina. Neuron 4, 461–467.

Yanagi, Y., Masuhiro, Y., Mori, M., Yanagisawa, J., Kato, S., 2000. p300/CBP acts as a coactivator of the cone-rod homeobox transcription factor. Biochem. Biophys. Res. Commun. 269, 410–414.

Young, R.W., 1985. Cell differentiation in the retina of the mouse. Anat. Rec. 212, 199–205.